Supporting Information

The mechanism behind enhanced reactivity of unsaturated phosphorus(V) electrophiles towards thiols

Yerin Park,†[ab] Alice L. Baumann,†[cd] Hyejin Moon,[ab] Stephen Byrne,[cd] Marc-André Kasper,[cd] Songhwan Hwang,[c] Han Sun,*[c] Mu-Hyun Baik*[ba] and Christian P. R. Hackenberger*[cd]

[a]Department of Chemistry, Korea Advanced Institute of Science and Technology (KAIST), Daejeon 34141, Republic of Korea

[b]Center for Catalytic Hydrocarbon Functionalizations, Institute for Basic Science (IBS), Daejeon 34141, Republic of Korea

[c]Chemical Biology Department, Leibniz-Forschungsinstitut für Molekulare Pharmakologie (FMP), Robert-Rössle-Strasse 10, 13125 Berlin, Germany

[d]Department of Chemistry, Humboldt Universität zu Berlin, Brook-Taylor-Straße 2, 12489 Berlin, Germany

*Corresponding authors. E-mail: hsun@fmp-berlin.de, mbaik2805@kaist.ac.kr, hackenbe@fmp-berlin.de

†These authors contributed equally to this work.

Table of Contents

1. Materials and Methods

Chemicals and solvents

Chemicals were purchased from Merck (Merck group, Germany), Bachem (Bachem holding AG, Switzerland), and Biomol (Biomol GmbH, Germany) and used without further purification. Dry solvents were purchased from Acros Organics (Thermo Fisher Scientific, USA).

Flash and thin-layer chromatography

Flash column chromatography was performed using NORMASIL 60® silica gel (40-63 µm, VWR international, USA) or high-purity grade silica gel (Davisil Grade 633, pore size 60 Å, 200-425 mesh particle size, Sigma-Aldrich Co., USA). Aluminium TLC plates (silica gel 60 coated with fluorescent indicator UV254) were purchased from Macherey-Nagel (Macherey-Nagel GmbH & Co. Kg, Germany). Spots were visualized by fluorescence depletion with a 254 nm lamp or manganese staining (10 g K_2CO_3, 1.5 g $KMnO_4$, 0.1 g NaOH in 200 mL H_2O), followed by heating.

Semipreparative HPLC

Semipreparative HPLC was performed on a Shimadzu prominence HPLC system (Shimadzu Corp., Japan) with a CBM20A communication bus module, a FRC-10A fraction collector, 2 pumps LC-20AP, and a SPD-20A UV/VIS detector, using a VP250/21 Macherey-Nagel Nucleodur C18 HTec Spum column (Macherey-Nagel GmbH & Co. Kg, Germany). Eluents: A = H_2O + 0.1% TFA, B = MeCN + 0.1% TFA.

High-resolution MS

High-resolution ESI-MS spectra were recorded on two different instruments: 1) Agilent 6220 TOF Accurate Mass coupled to an Agilent 1200 LC (Agilent Technologies, USA). On this system, samples were measured at 35 °C between 100-2000 m/z. The used column was an Accucore RP-MS (30 x 2.1 mm; 2.6 mm particle size) eluted with a flow of 0.8 mL/min and the following gradient (A = H_2O + 0.1% TFA, B = MeCN + 0.1% TFA): 5% B 0-0.2 min, 5-99% B 0.2-1.1 min, 99% B 1.1-2.5 min. 2) Agilent Technologies 6230 Accurate Mass TOF LC/MS linked to Agilent Technologies HPLC 1260 Series; Column: Thermo Accucore RP-MS; Particle Size: 2.6 mm; Dimension: 30 x 2.1 mm. The following gradient was used (A = H_2O + 0.1% formic acid, B = MeCN + 0.1% formic acid): 5% B 0.0-0.2 min, 5-99% B 0.2-1.1 min, 99% B 1.1-3.6 min, 5% B 3.6-4.9 min. Flow rate: 0.8 mL/min; UV-detection: 220 nm, 254 nm, 300 nm.

NMR

NMR spectra were recorded with a Bruker AV-III 300 MHz spectrometer and a Bruker AV III 600 MHz spectrometer, both equipped with a broadband probe (BBFO). Chemical shifts δ for ^{1}H and ^{13}C NMR spectra are reported in ppm relative to residual solvent peaks ($CDCl_3$: 7.26 [ppm]; DMSO-d_6: 2.50 [ppm]; CD_3CN: 1.94 [ppm]; D_2O: 4.79 [ppm] for ^{1}H-spectra and $CDCl_3$: 77.16 [ppm]; DMSO-d_6: 39.52 [ppm]; CD_3CN 1.32 [ppm] for ^{13}C-spectra).

Analytical HPLC

Analytical HPLC for thiol addition kinetic measurements was conducted on a Shimadzu prominence HPLC system (Shimadzu Corp., Japan) with a CBM-20A communication bus module, a SIL-20A autosampler, 2 pumps LC-20AT, and a SPD-M20A UV/VIS detector, a CTO-20A column oven and a RF-10AXL fluorescence detector, using an Agilent Eclipse C18 5 µm, 250 x 4.6 mm RR-HPLC column (Agilent Technologies, USA) with a flow rate of 1.0 mL/min. The following gradients were used (A = H_2O + 0.1% TFA, B = MeCN + 0.1% TFA): 2% B 0-5 min, 2-45% B 5-35 min, 45-95% B 35-36 min, 95% B 36-40 min, 95 to 2% B 40-41 min, 2% B 41-45 min. Fluorescence spectra with Ex/Em 336/490 nm were recorded.

2. Chemical Synthesis

1-Ethoxy-1-ethynyl-*N*,*N*-diisopropylphosphanamine (1)

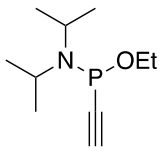

A flame-dried round bottom Schlenk flask was charged with phosphorus trichloride (Sigma, 12.5 mmol, 1090 µL, 1.0 eq.) and dry ether (50 mL) under an argon atmosphere and cooled to –30 °C in an acetone/dry ice bath. Ethanol (12.5 mmol, 728 µL, 1.0 eq.) and triethylamine (12.5 mmol, 1.733 mL, 1.0 eq.) were added, and the solution was stirred at –30 °C for 10 min before warming to r.t. and stirred for another hour. The resulting white suspension was quickly filtered over celite. The filtrate was collected in a flame-dried round bottom Schlenk flask and cooled again to –30 °C under an argon atmosphere. Diisopropylamine (25 mmol, 3.528 mL, 2.0 eq.) was added, and the reaction mixture was stirred at –30 °C for 10 min before warming up to r.t. and stirred for another hour. The resulting suspension was filtered over celite again. The clear filtrate was cooled to –78 °C under an argon atmosphere and a solution of ethynylmagnesium bromide (Sigma, 0.5 M in THF, 13.75 mmol, 27.5 mL, 1.1 eq.) was added, stirred for 10 min at –78 °C and then at r.t. for another hour. The reaction mixture was then concentrated to roughly 20 mL under reduced pressure, diluted with saturated aqueous $NaHCO_3$ (60 mL), and extracted with EtOAc (3x 120 mL). The combined organic layers were dried over $NaSO_4$, filtered, and the solvents were removed under reduced pressure. The resulting oily residue was purified by silica gel chromatography (*n*-hexane + 1% Et_3N) using high-purity grade silica gel (Davisil Grade 633, pore size 60 Å, 200-425 mesh particle size, Sigma-Aldrich Co., USA). After evaporating the solvents under reduced pressure, the titled compound **1** was obtained as a yellow oil (1.236 g, 6.14 mmol, 49%). ^{1}H-NMR: (300 MHz, CD_3CN): δ = 3.77-3.63 (m, 4H), 3.33 (d, *J* = 1.8 Hz, 1H), 1.21-1.13 (m, 15H). ^{13}C-NMR: (75 MHz, CD_3CN): δ = 92.75 (d, *J* = 7.4 Hz), 86.67 (d, *J* = 18.5 Hz), 62.86 (d, *J* = 16.20 Hz), 48.36, 24.37, 17.40 (d, *J* = 7.5 Hz). ^{31}P-NMR (122 MHz, CD_3CN): δ = 92.22. HR-MS (ESI+) for $C_{10}H_{20}NOPNa^+$ [M+Na^+] calcd.: 224.1175, found: 224.1270.

***S*-Boc-ethylamine *O*-ethyl ethynylphosphonothiolate (4)**

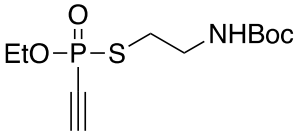

A round bottom flask was charged with **1** (93 mg, 0.465 mmol, 1.0 eq.), dissolved in 5 mL dry acetonitrile and cooled to –40 °C in an acetone/dry ice bath. Separately, a solution of *tert*-butyl (2-mercaptoethyl)carbamate **2**[1] {El-Gendy, 2013 #1} (82 mg, 0.465 mmol, 1.0 eq.) and tetrazole (Sigma, 0.45 M in MeCN, 2.07 mL, 0.93 mmol, 2.0

eq.) was prepared and added dropwise to the first stirred solution at –40 °C. The reaction mixture was stirred for 10 min at –40 °C before allowed to warm to r.t. and stirred for another 30 min. Then, a *tert*-butyl hydroperoxide solution (Sigma, 70 wt. % in H_2O, 133 mL, 0.465 mmol, 1.0 eq.) was added at r.t. and stirred for 10 min. The reaction mixture was then diluted with H_2O (1.5 mL) and extracted with DCM (3x 5 mL). The combined organic layers were dried over Na_2SO_4, filtered and the solvents were removed under reduced pressure. Purification by silica gel chromatography (100% EtOAc) gave the desired compound as a colourless oil (44 mg, 0.15 mmol, 32%). ^{1}H-NMR: (600 MHz, DMSO-d_6): δ = 7.07 (t, *J* = 5.4 Hz, 1H), 4.83 (d, *J* = 12.7 Hz, 1H), 4.17-4.11 (m, 2H), 3.23-3.20 (m, 2H), 2.91 (dt, *J* = 15.5, 6.9 Hz, 2H), 1.38 (s, 9H), 1.30 (t, *J* = 7.0 Hz, 3H). ^{13}C-NMR: (151 MHz, DMSO-d_6): δ = 155.42, 93.47 (d, *J* = 40.6 Hz), 77.93, 76.34, 63.18 (d, *J* = 6.7 Hz), 40.19, 30.01, 28.15, 15.86 (d, *J* = 7.1 Hz). ^{31}P-NMR (243 MHz, DMSO-d_6): δ = 11.75. HR-MS (ESI+) for $C_{11}H_{20}NO_4PSNa^+$ [M+Na^+] calcd.: 316.0743; found: 316.0746.

_O_-Boc-ethylamine _O_-ethyl ethynylphosphonate (5)

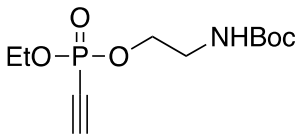

A round bottom flask was charged with **1** (201 mg, 1.0 mmol, 1.0 eq.), dissolved in 10 mL dry acetonitrile and cooled to −40 °C. Separately, a solution of Boc-protected ethanolamine **3**[2]. (161 mg, 1.0 mmol, 1.0 eq.) and tetrazole (Sigma, 0.45 M in MeCN, 4.4 mL, 2.0 mmol, 2.0 eq.) was prepared and added dropwise to the first stirred solution at −40 °C. The reaction mixture was stirred for 10 min at −40 °C before allowed to warm to r.t. and stirred for another 30 min. Then, a *tert*-butyl hydroperoxide solution (Sigma, 70 wt. % in H_2O, 286 mL, 1.0 mmol, 1.0 eq.) was added at r.t. and stirred for 10 min. The reaction mixture was then diluted with 30 mL H_2O and extracted with DCM (3 times 60 mL). The combined organic layers were dried over Na_2SO_4, filtered and the solvents were removed under reduced pressure. After purification by silica gel chromatography (100% EtOAc) the titled product was obtained as a colourless oil (168 mg, 0.60 mmol, 60%). ^{1}H-NMR: (300 MHz, $CDCl_3$): δ = 5.19 (t, *J* = 6.1 Hz, 1H), 4.16 – 3.95 (m, 4H), 3.30 (q, *J* = 5.5 Hz, 2H), 3.05 (d, *J* = 13.4 Hz, 1H), 1.31 (s, 9H), 1.26 (td, *J* = 7.1, 0.8 Hz, 3H). ^{13}C-NMR: (75 MHz, $CDCl_3$): δ = 155.85, 88.69 (d, *J* = 51.1 Hz), 79.68, 73.76 (d, *J* = 292 Hz), 66.65 (d, *J* = 6.5 Hz), 63.92 (d, *J* = 5.5 Hz), 40.78 (d, *J* = 7.2 Hz), 28.41, 16.09 (d, = 7.0 Hz). ^{31}P-NMR: (122 MHz, $CDCl_3$): δ = -8.03. HR-MS (ESI+) for $C_{11}H_{21}NO_5P^+$ [M+H^+] calcd.: 278.1152, found: 278.1149.

4-Oxo-4-((2-((5-sulfonaphthalen-1-yl)amino)ethyl)amino)butanoic acid (6)

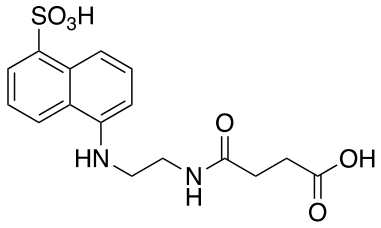

HATU (Bachem, 690 mg, 1.814 mmol, 1.0 eq.) and succinic acid (214 mg, 1.814 mmol, 1.0 eq.) were dissolved in 6 mL DMF containing DIPEA (1.263 mL, 7.254 mmol, 4.0 eq.). This solution was added to EDANS (Biomol, sodium salt, 483 mg, 1.814 mmol, 1.0 eq.) dissolved in 3 mL DMF and the mixture was stirred at r.t. for 30 min. The solvents were then removed under reduced pressure and the crude product was purified by semi-preparative HPLC (gradient: 5-90% MeCN + 0.1% TFA in H_2O + 0.1% TFA over 60 min, flow: 10 mL/min), giving product **6** (508 mg, 1.387 mmol, 76%) as a slightly greenish powder after lyophilization. HR-MS (ESI+) for $C_{16}H_{19}N_2O_6S^+$ [M+H$^+$] calcd.: 367.0959, found: 367.0954.

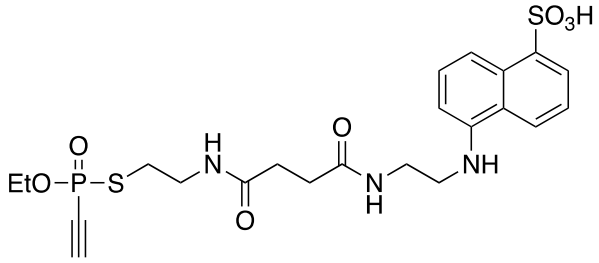

***S*-EDANS *O*-ethyl ethynylphosphonothiolate (7)**

First, Boc-protected ethynylphosphonothiolate derivative **4** (17 mg, 0.0580 mmol, 1.0 eq.) was dissolved in TFA/H_2O = 95:5 at a concentration of 0.1 M. The solution was stirred for 10 min at r.t. and then diluted with water (1:10). The deprotected amine (an oil) was obtained quantitatively (11.2 mg, 0.0580 mmol) after lyophilization and was used in the subsequent step without further purification.

Secondly, a solution containing HATU (Bachem, 24.2 mg, 0.0637 mmol, 1.1 eq.), carboxylic acid EDANS-derivative **6** (23.3 mg, 0.0637 mmol, 1.1 eq.) and DIPEA (30 µL, 0.174 mmol, 3.0 eq.) in 0.2 mL DMF was added to the crude amine from the first step (11 mg, 0.0578 mmol, 1.0 eq., dissolved in 0.1 mL DMF) and the mixture was stirred at r.t. for 30 min. The solvents were then evaporated under reduced pressure and the crude product was purified via semi-preparative HPLC (gradient: 10-50% MeCN + 0.1% TFA in H_2O + 0.1% TFA over 50 min, flow: 5 mL/min) giving product **7** (10 mg, 0.0185 mmol, 32%) as a white powder after lyophilization. ^{1}H-NMR: (600 MHz, DMSO-d_6): δ = 8.40 (m, broad, 1H), 8.16-8.09 (m, 2H), 8.07 (d, *J* = 8.5 Hz, 1H), 8.01-7.95 (m, 1H), 7.45-7.40 (m, 1H), 7.39-7.34 (m, 1H), 6.93 (m, broad, 1H), 4.83 (d, *J* = 12.8 Hz, 1H), 4.13 (dq, *J* = 10.1, 7.0 Hz, 2H), 3.41 (q, *J* = 6.1 Hz, 2H), 3.36-3.29 (m, 4H), 3.11-3.04 (m, 1H), 2.92 (dtd, *J* = 16.2, 6.9, 2.7 Hz, 2H), 2.38-2.32 (m, 4H), 1.29 (t, *J* = 7.1 Hz, 3H), 1.16 (t, *J* = 7.3 Hz, 1H). ^{13}C-NMR: (151 MHz, DMSO-d_6): δ = 172.22,

171.59, 144.19, 130.09, 125.90, 124.71, 124.35, 124.21, 123.80, 123.60, 123.40, 122.66, 93.55 (d, *J* = 41.8 Hz), 77.12 (d, *J* = 232.1 Hz), 63.29 (d, *J* = 6.6 Hz), 45.78, 38.94 (d, *J* = 5.4 Hz), 37.05, 30.65 (d, *J* = 12.5 Hz), 29.70, 15.90 (d, *J* = 7.2 Hz), 8.61. ^{31}P-NMR (243 MHz, DMSO-d_6): δ = 11.77. HR-MS (ESI+) for $C_{22}H_{29}N_3O_7PS_2^+$ [M+H$^+$] calcd.: 542.1179, found: 542.1156.

_O_-EDANS _O_-ethyl ethynylphosphonate (8)

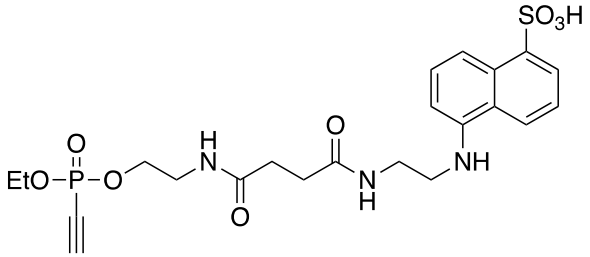

First, Boc-protected ethynylphosphonate **5** (22 mg, 0.079 mmol) was dissolved in TFA/H_2O = 95:5 at a concentration of 0.1 M. The solution was stirred for 10 min at r.t. and subsequently diluted with water (1:10). The deprotected amine (an oil) was obtained quantitatively (14 mg, 0.079 mmol) after lyophilization and was used in the subsequent step without further purification.

Then, a solution containing HATU (Bachem, 33.2 mg, 0.087 mmol, 1.1 eq.), carboxylic acid EDANS-derivative **6** (32 mg, 0.087 mmol, 1.1 eq.) and DIPEA (47 µL, 0.237 mmol, 3.0 eq.) in 0.2 mL DMF was added to the crude amine from the first step (14 mg, 0.079 mmol, 1.0 eq., dissolved in 0.1 mL DMF) and the mixture was stirred at r.t. for 30 min. The solvents were then evaporated under reduced pressure and the crude product was purified via semipreparative HPLC (gradient: 10-50% MeCN + 0.1% TFA in H_2O + 0.1% TFA over 50 min, flow: 5 mL/min) giving product **8** (13 mg, 0.0248 mmol, 31%) as a white powder after lyophilization. ^{1}H-NMR: (600 MHz, DMSO-d_6): δ = 8.27 (d, *J* = 8.6 Hz, 1H), 8.13-8.04 (m, 3H), 7.96-7.94 (m, 1H), 7.82 (s, broad, 1H), 7.40-7.29 (m, 2H), 6.76 (d, *J* = 7.4 Hz, 1H), 4.55 (d, *J* = 13.5 Hz, 1H), 4.08 (dq, *J* = 9.0, 7.1 Hz, 2H), 3.99-3.95 (m, 2H), 3.39 (q, *J* = 6.1 Hz, 2H), 3.32-3.28 (m, 4H), 2.39-2.32 (m, 4H), 1.27 (t, *J* = 7.1 Hz, 3H). ^{13}C-NMR: (151 MHz, DMSO-d_6): δ = 172.16, 171.74, 144.25, 130.11, 125.94, 125.58, 124.07, 124.05, 123.38, 123.23, 123.12, 122.61, 92.55 (d, *J* = 48.8 Hz), 73.81 (d, *J* = 284.5 Hz), 65.12 (d, *J* = 6.0 Hz), 63.23 (*J* = 5.7 Hz), 53.61, 30.65 (d, *J* = 14.8 Hz), 18.07, 16.72, 15.82 (d, *J* = 6.7 Hz), 12.47. ^{31}P-NMR: (243 MHz, DMSO-d_6): δ = −8.36. HR-MS (ESI+) for $C_{22}H_{29}N_3O_8PS^+$ [M+H$^+$] calcd.: 526.1408, found: 526.1387.

_O_,S-Diethyl ethynylphosphonothiolate (13)

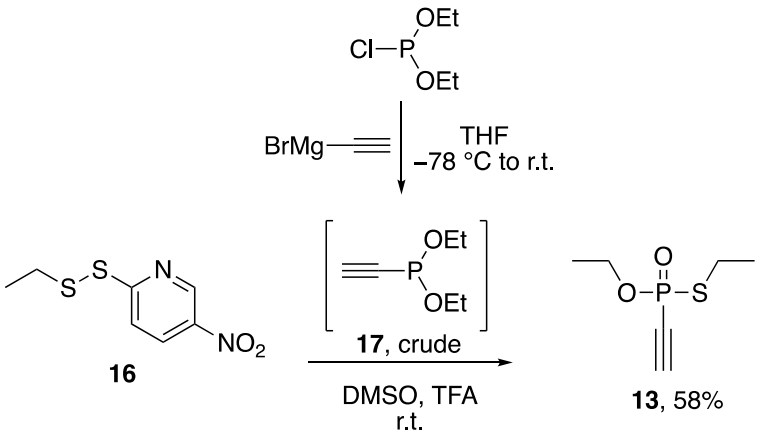

Scheme S1 Synthesis of ethynylphosphonothiolate.

Ethynylphosphonothiolate **13** was synthesized from electrophilic disulfide **16** and ethynylphosphonite **17** according to Scheme S1 adapting a previously published protocol.[3]

First, a Schlenk-flask was charged with diethyl chlorophosphite (Sigma, 278 µL, 2.00 mmol) under an argon atmosphere, cooled to –78 °C in an acetone/dry-ice bath and ethynylmagnesium bromide solution (Sigma, 0.5 M in THF, 4.40 mL, 2.20 mmol) was added dropwise and stirred for 10 min at –78 °C. The solution was allowed to warm to r.t., analyzed by ^{31}P-NMR (122 MHz, crude in THF, δ = 128.02 ppm) and was used in the next step without further dilution or purification.

Second, electrophilic disulfide **16**[3] (100 mg, 0.462 mmol, 1.0 eq.) was dissolved in dry DMSO (4.6 mL) containing trifluoroacetic acid (353 µL, 4.62 mmol, 10 eq.). To this stirred mixture was added dropwise the above described ethynylphosphonite solution (crude in THF, ca. 0.427 M, 2.16 mL, 0.924 mmol, 2.0 eq.) at r.t. After 5 min stirring at r.t., the crude reaction mixture was directly loaded on a silica gel column (gradient: *n*-hexane/EtOAc = 2:1 to 100% EtOAc) and the ethynylphosphonothiolate product **13** was isolated as a colourless oil (48 mg, 0.270 mmol, 58%). ^{1}H-NMR: (300 MHz, $CDCl_3$): δ = 4.24 (dq, *J* = 9.6, 7.1 Hz, 2H), 3.17 (d, *J* = 12.5 Hz, 1H), 3.07-2.87 (m, 2H), 1.41 (td, *J* = 7.2, 5.9 Hz, 6H). ^{13}C-NMR: (75 MHz, $CDCl_3$): δ = 89.23 (d, *J* = 42.8 Hz), 77.33 (d, *J* = 236.9 Hz), 63.93 (d, *J* = 6.8 Hz), 25.72 (d, *J* = 3.7 Hz), 16.21 (d, *J* = 7.4 Hz), 16.12 (d, *J* = 6.4 Hz). ^{31}P-NMR (122 MHz, $CDCl_3$): δ = 17.40. HR-MS (ESI+) for $C_6H_{12}O_2PS^+$ [M+H$^+$] calcd.: 179.0290, found: 179.0301.

3. Determination of Second-order Rate Constants

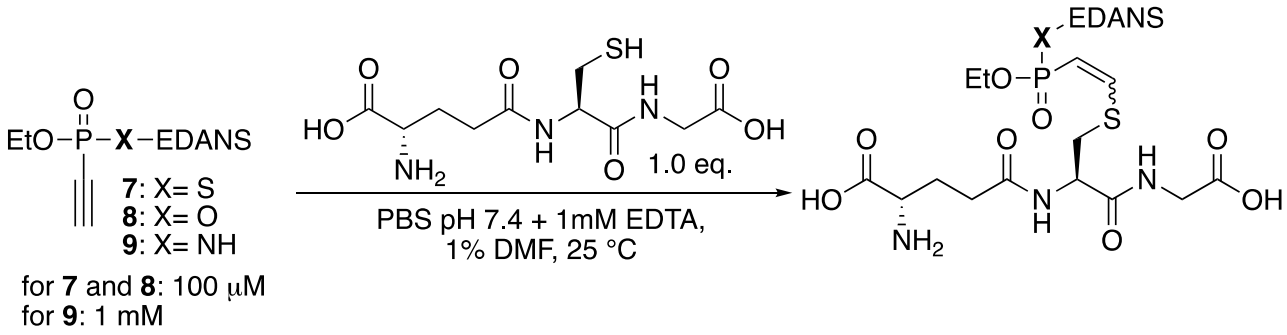

Scheme S2 General reaction conditions of the addition of glutathione to P(V) electrophiles.

Reactions were performed in a volume of 0.5 mL in 1.5 mL Eppendorf tubes on a thermoshaker at 25 °C, following our previously published protocol.[4] Glutathione additions to EDANS-P(V)-electrophiles **7** (X=S) and **8** (X=O) were conducted at 100 µM. For the less reactive derivative **9** (X=NH), the reaction was conducted at 1 mM. Therefore, 2.5 µL of either a 20 mM or a 200 mM solution of EDANS-P(V) electrophile in DMF and 5 µL of a 10 mM or a 100 mM solution of unconjugated EDANS (internal standard) in 1:1 DMF/conjugation buffer* were added to 488 µL conjugation buffer. Then, 5 µL of a 10 mM or a 100 mM solution of reduced glutathione (GSH) in conjugation buffer was added to start the reaction. The first sample (t= 0 min) was drawn before the addition of glutathione. Samples were drawn in a volume 2 µL (for the reaction at 1 mM) or 20 µL (for the reactions at 100 mM) and immediately diluted into 98 µL or 80 µL of 50 mM NaOAc buffer at pH 3.5 to stop the reaction. Samples were subjected to fluorescent HPLC analyses, injecting 20 µL each of the quenched reaction mixture. *conjugation buffer: phosphate buffered saline (KCl [200 mg/L], KH_2PO_4 [200 mg/L], NaCl [8000 mg/L], Na_2HPO_4) + 1 mM EDTA. The buffer was adjusted to pH=7.4 using NaOH.

Signal intensities of P(V) electrophile starting material (SM) and the internal standard EDANS (Std) were quantified by integration of the area under the peaks. The concentration of remaining starting material at time point x ($[SM]_x$) was calculated as follows:

$$[SM]_x = \frac{\frac{SM_x}{Std_x}}{\frac{SM_0}{Std_0}} \cdot [SM]_0$$

whereas SM and Std are the measured intensities of the respective peaks at a given time point and $[SM]_0$ is the initial concentration of P(V) electrophiles (either 1 mM or 100 µM). The inverse molar concentrations of the remaining P(V) electrophile were plotted against time. Second-order rate constants (*k)* were determined from the slopes of the linear plots through the mean values of three independent measurements, based on the following mathematical consideration:

$$v = k \cdot [SM] \cdot [GSH] = \frac{d[SM]}{dt}$$

$$if\ [SM] = [GSH]$$

$$\frac{d[SM]}{dt} = k \cdot [SM]^2$$

$$\frac{d[SM]}{[SM]^2} = k\ dt$$

$$\frac{1}{[SM]} = k\ t + \frac{1}{[SM]_0}$$

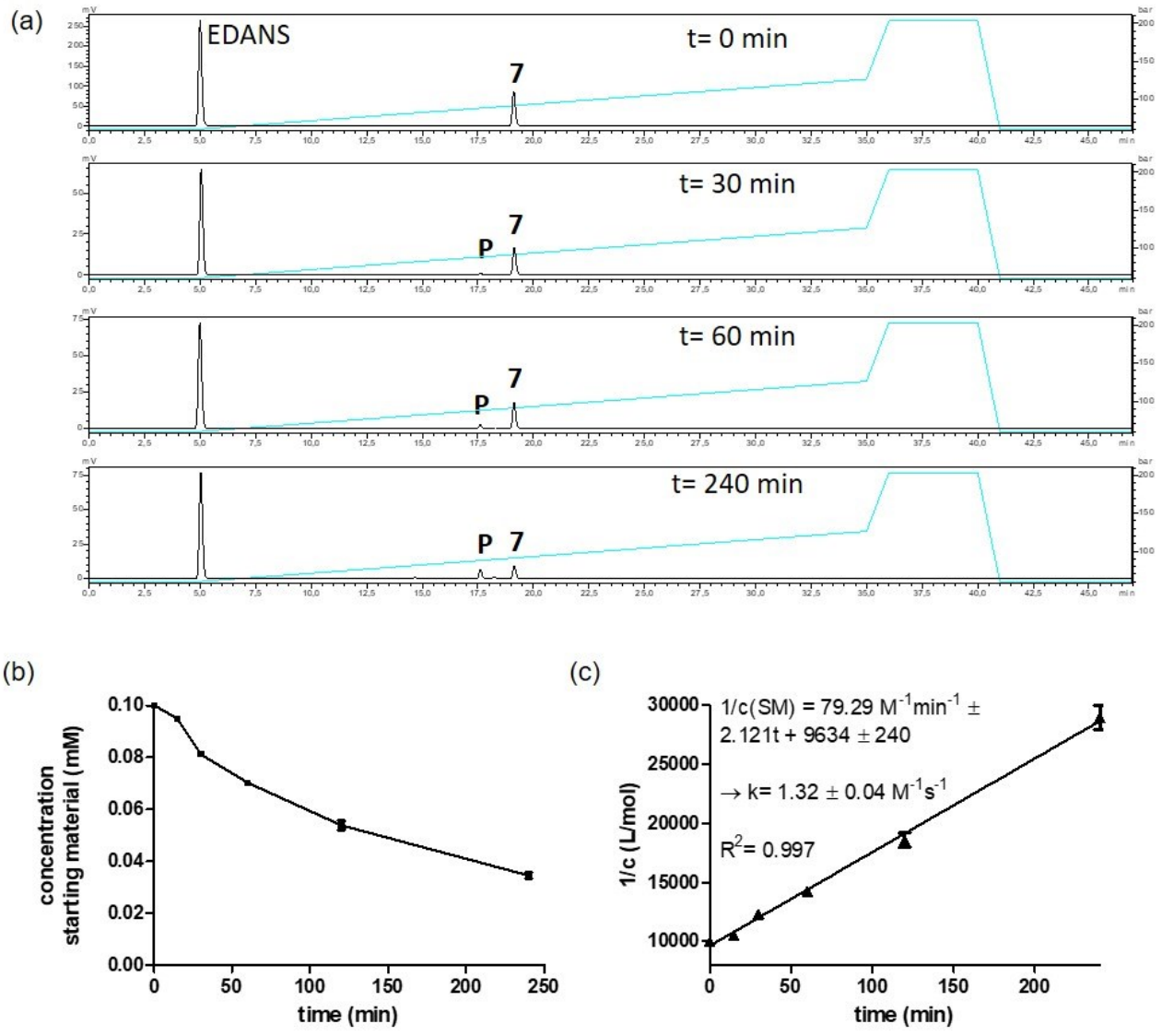

Fig. S1 (a) HPLC traces of the reaction mixture at the indicated time points. **P** = glutathione-addition product. (b) Concentration of starting material **7** (ethynylphosphonothiolate) over time. Shown are the mean and standard

deviation of three independent measurements. (c) 1/c (c = concentration) over time and linear plot. The slope is the second-order rate constant. Shown are the mean and standard deviation of three independent measurements.

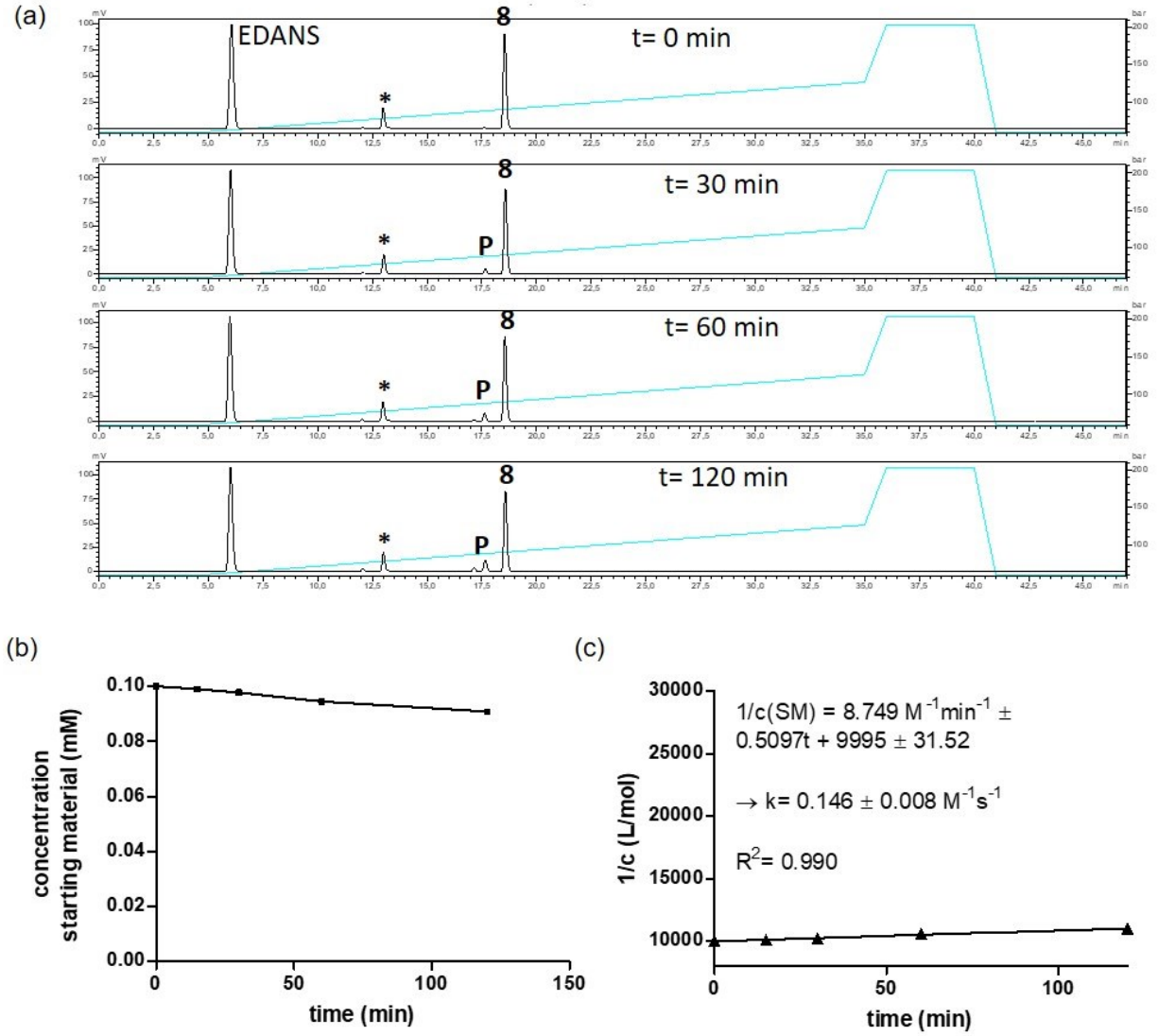

Fig. S2 (a) HPLC traces of the reaction mixture at the indicated time points. **P** = glutathione-addition product. *EDANS-related impurity; no influence on the kinetics expected (b) Concentration of starting material **8** (ethynylphosphonate) over time. Shown are the mean and standard deviation of three independent measurements. (c) 1/c (c = concentration) over time and linear plot. The slope is the second-order rate constant. Shown are the mean and standard deviation of three independent measurements.

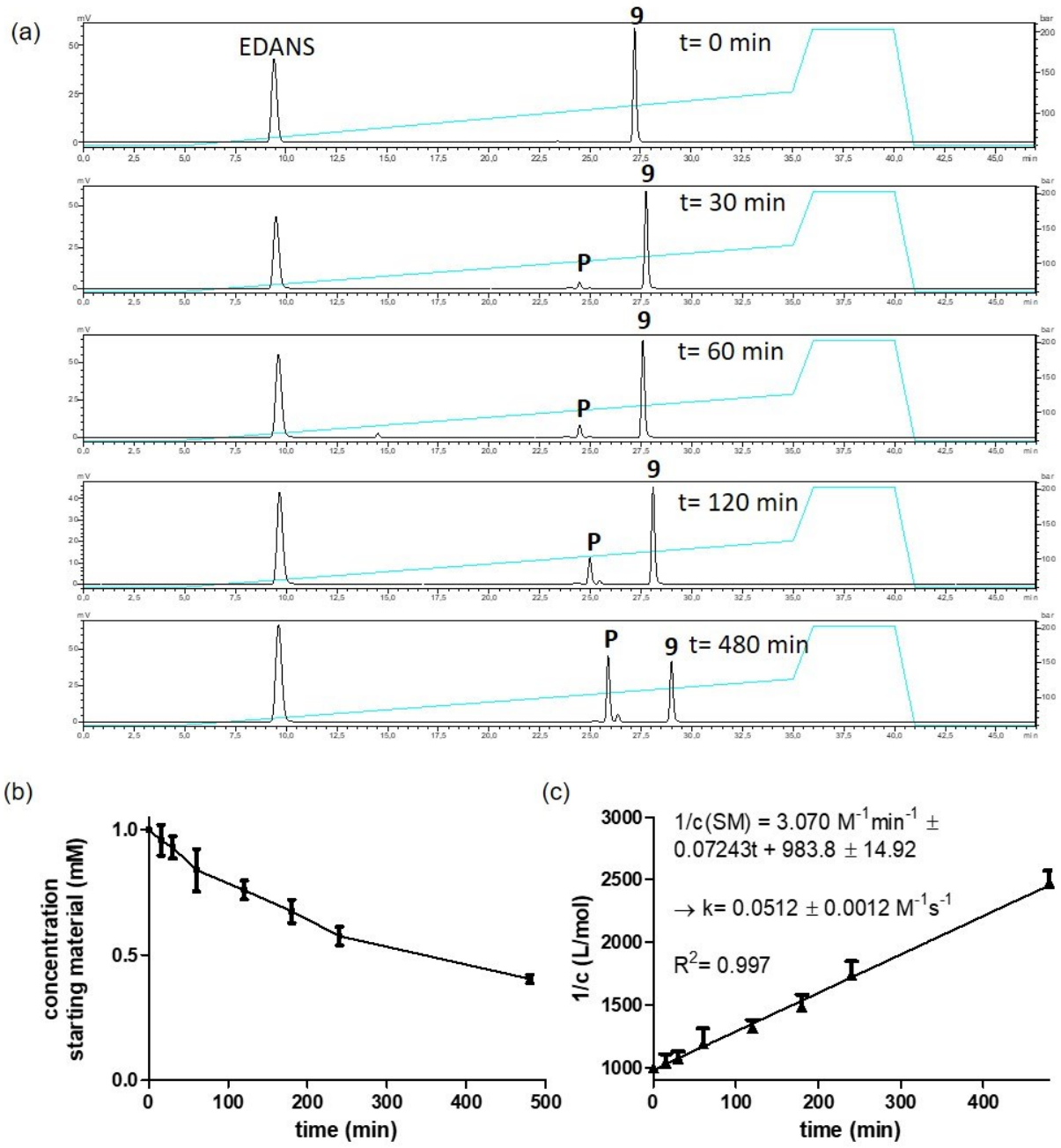

Fig. S3 (a) HPLC traces of the reaction mixture at the indicated time points. **P** = glutathione-addition product. (b) Concentration of starting material **9** (ethynylphosphonamidate) over time. Shown are the mean and standard deviation of three independent measurements. (c) 1/c (c = concentration) over time and linear plot. The slope is the second-order rate constant. Shown are the mean and standard deviation of three independent measurements.

4. Stereoselectivity for Thiol Addition to Ethynylphosphonothiolate

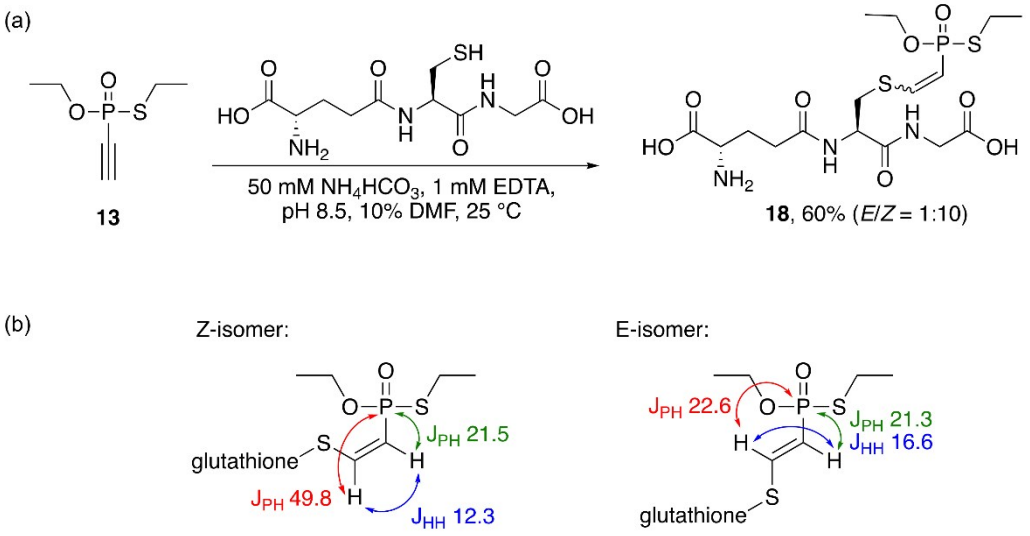

Fig. S4 (a) Reaction conditions of glutathione addition to ethynylphosphonothiolate **13**. (b) Observed coupling constants in Hertz for the two regioisomers.

In order to investigate the regioselectivity of the thiol addition to ethynylphosphonothiolates, glutathione was reacted with ethynylphosphonothiolate **13** (Fig. S4a).

Reduced glutathione (141 mg, 0.460 mmol, 2.0 eq.) was dissolved in 10.35 mL aqueous 50 mM NH_4HCO_3 buffer at pH 8.5 containing 1 mM EDTA and added to a solution of ethynylphosphonothiolate **13** (41 mg, 0.230 mmol, 1.0 eq.) in 1.15 mL DMF and the mixture was stirred at r.t. for 90 min. The solvents were then removed under reduced pressure and the residue was redissolved in 5 mL H_2O and purified via semipreparative HPLC (gradient: 5-90% MeCN + 0.1% TFA in H_2O + 0.1% TFA over 40 min, flow: 10 mL/min). The two regioisomers could be separated and were analyzed separately by NMR. The *E*- and *Z*-isomers were thereby assigned based on characteristic J_{HH} and J_{PH} coupling constants (Fig. S4b), which are similar to reported coupling constants for phosphonamidates[4] and phosphonates[5]: *E*-isomer of **18** (6 mg, 0.0124 mmol, 5%) and *Z*-isomer of **18** (61 mg, 0.1256 mmol, 55%).

Z-isomer of **18**:

^{1}H-NMR: (600 MHz, D_2O): δ = 7.53 (ddd, *J* = **49.8**, **12.3**, 2.4 Hz, 1H), 5.97 (dt, *J* = **21.5**, **12.3** Hz, 1H), 4.70 (ddd, *J* = 20.1, 8.6, 5.2 Hz, 1H), 4.23 (dq, *J* = 9.3, 7.1 Hz, 2H), 4.08 (td, *J* = 6.6, 1.5 Hz, 1H), 4.04 (s, 2H), 3.43 (ddd, *J* = 14.4, 5.2, 3.8 Hz, 1H), 3.23 (dt, *J* = 14.4, 8.5 Hz, 1H), 2.92-2.82 (m, 2H), 2.66-2.58 (m, 2H), 2.30-2.21 (m, 2H), 1.38 (t, *J* = 7.1 Hz, 3H), 1.35 (td, *J* = 7.4, 4.3 Hz, 3H). ^{13}C-NMR (151 MHz, D_2O): δ = 176.89, 175.55, 174.60 (d, *J* = 11.6 Hz), 174.4, 165.64 (q, *J* = 35 Hz), 154.88 (d, *J* = 17.9 Hz), 119.06 (q, *J* = 292 Hz, acetonitrile contamination), 116.15 (dd, *J* = 148.6, 30.3 Hz), 66.04 (dd, *J* = 10.1, 6.9 Hz), 56.36 (d, *J* = 6.7 Hz), 55.12, 43.91, 39.08 (d, *J* = 11.0 Hz), 33.79, 28.28 (d, *J* = 6.0 Hz), 27.40, 18.30. ^{31}P-NMR: (243 MHz, D_2O): δ = 44.92. 44.88 (two diastereoisomers). HR-MS (ESI+) for $C_{16}H_{29}N_3O_8PS_2^+$ [M+H$^+$] calcd.: 486.1128, found: 486.1605.

E-isomer of **18**:

^{1}H-NMR: (600 MHz, D_2O): δ = 7.57 (dd, *J* = **22.6**, **16.6** Hz, 1H), 6.08 (ddd, *J* = **21.3**, **16.6**, 1.4 Hz, 1H), 4.78-4.75 (m, 1H, overlaps with solvent signal), 4.23 (dq, *J* = 9.3, 7.1 Hz, 2H), 4.06 (s, 2H), 4.00 (t, *J* = 6.5 Hz, 1H), 3.46 (dd, *J* = 14.4, 5.5 Hz, 1H), 3.29 (ddd, *J* = 14.4, 7.9, 1.6 Hz, 1H), 2.91-2.80 (m, 2H), 2.66-2.54 (m, 2H), 2.24 (q, *J* = 8.1, 7.7 Hz, 2H), 1.39 (t, *J* = 7.1 Hz, 3H), 1.35 (t, *J* = 7.4 Hz, 3H). ^{13}C-NMR (151 MHz, D_2O): δ = 177.19, 175.66, 175.15, 174.57, 165.58, 152.82 (d, *J* = 9.7 Hz), 115.13 (d, *J* = 151 Hz), 66.28 (d, *J* = 5.9 Hz), 55.66, 55.22, 43.96, 35.52, 33.79, 28.38, 27.45, 18.24 (d, *J* = 6.3 Hz). ^{31}P-NMR: (243 MHz, D_2O): δ = 45.27, 45.23 (two diastereoisomers). HR-MS (ESI+) for $C_{16}H_{29}N_3O_8PS_2^+$ [M+H$^+$] calcd.: 486.1128, found: 486.1605.

5. Computational Details

5.1 Molecular electrostatic potential

The initial structures of the molecules (vinylphosphonothiolate **10**, vinylphosphonate **11**, vinylphosphonamidate **12**, ethynylphosphonothiolate **13**, ethynylphosphonate **14,** and ethynylphosphonamidate **15**) were built using GaussView6.[6] Geometry optimizations of the molecules were performed using the density functional theory (DFT)[7] implemented in Gaussian 16[8] at the B3LYP[9]–[13]/aug-cc-pVTZ[14],[15] level of theory in combination with the IEFPCM solvation model[16] for water (ε = 78.4). The molecular electrostatic potential was evaluated at each point on the isodensity surface with a value of 0.0004 a.u.

5.2 Reaction energy profile

Density functional theory (DFT) calculations for minimum energy structures and energy profiles were conducted using the Jaguar 9.1 suite of programs.[17] Geometry optimizations and transition state calculations were carried out employing the University of Minnesota Functionals meta-hybrid DFT exchange-correlation functional (M06-2X)[18] with the 6-31G** basis set.[19] The Poisson-Boltzmann solver, as implemented in Jaguar 9.1, was employed to obtain the minimum-energy solvated structures along with the solvation energies in the aqueous solution. The molecular systems in the aqueous environment were treated with the self-consistent reaction field (SCRF) approach[20],[21],[22] with a proper dielectric constant ε = 78.4. For continuum models, atomic radii for the generation of the solute surface are subject to empirical parameterization. The standard set of optimized radii was used for H (1.150 Å), C (1.900 Å), N (1.600 Å), O (1.600 Å), P (2.074 Å), S (1.900 Å) as implemented in Jaguar.[23] With the solution-phase optimized structures, single-point calculations were executed with the triple-ζ quality of the basis set, cc-pVTZ(-f)[24], in order to reevaluate the gas-phase electronic energies. Frequency calculations were computed at the same level as the geometry optimizations to obtain the zero-point energy (ZPE) and entropy. Gibbs free energy in the solution phase has been calculated from the energy components with the following protocol:

$$G(sol) = G(gas) + Gsolv \quad (1)$$

$$G(gas) = H(gas) - TS(gas) \quad (2)$$

$$H(gas) = E(SCF) + ZPE \quad (3)$$

$$\Delta E(SCF) = \Sigma E(SCF) \text{ for products} - \Sigma E(SCF) \text{ for reactants} \quad (4)$$

$$\Delta G(sol) = \Sigma G(sol) \text{ for products} - \Sigma G(sol) \text{ for reactants} \quad (5)$$

G(gas) is the free energy in gas phase; G(solv) is the free energy of solvation as computed using the continuum solvation model; G(sol) is the solution phase free energy; H(gas) is the enthalpy in gas phase; T is the

temperature (25 °C, 298.15 K); S(gas) is the entropy in gas phase; E(SCF) is the electronic energy as computed from the self consistent-field method; ZPE is the zero-point energy; Note that entropy refers to the vibrational, rotational, and translational entropy of the solute(s). The solvent entropies are implicitly incorporated in the continuum solvation model.

5.3 Consideration of ΔG_{pKa}

For calculating the step barrier $\Delta G^{\ddagger}_{calc}$, we supposed that the thiolate (EtS^-) participate in the nucleophilic addition instead of EtSH. In the DFT calculation, we treat the reaction as an equimolar reaction between EtS^- and electrophile. Thus, it is necessary to consider the equilibrium ratio of EtS^- in the reaction media in order to describe the experimentally observed rate. The Henderson–Hasselbalch equation would give the molar fraction between EtS^- and EtSH to be 1/1622.

$$pH = pKa + log(\frac{[EtS^-]}{[EtSH]})$$

$$\frac{[EtS-]}{[EtSH]} = 10^{pH-pKa} = \frac{1}{1622}$$

where the pKa of EtSH is 10.61 at 25 °C[25] and the pH of the PBS buffer solution is 7.4.

Thus, the predicted rate constant k_{calc} would be less than the actual rate constant k.

$$k_{calc} \propto \exp(\frac{-\Delta G^{\ddagger}_{calc}}{RT})$$

$$r = k \cdot [SM] \cdot [EtSH]$$
$$= k_{calc} \cdot [SM] \cdot [EtS^-]$$
$$= k_{calc} \cdot [SM] \cdot \frac{[EtSH]}{1622}$$

$$k = \frac{k_{calc}}{1622}$$

Instead of adjusting the rate constant k_{calc}, we can correct the energy barrier by including the free energy for forming the thiolate (ΔG_{pKa}). The actural $\Delta G^{\ddagger}$ could be reached by adding ΔG_{pKa} to $\Delta G^{\ddagger}_{calc}$ as below.

$$\Delta G_{pKa} = -RT \cdot ln\left(\frac{[EtS^-]}{[EtSH]}\right) = -\left(0.593\frac{kcal}{mol}\right) \cdot (298.15\ K) \cdot ln\left(\frac{1}{1622}\right) = 4.38\ kcal\ mol^{-1}$$

$$\Delta G^{\ddagger} = \Delta G^{\ddagger}_{calc} + \Delta G_{pKa}$$

$$\Delta G^{\ddagger} = \Delta G^{\ddagger}_{calc} + 4.38\ kcal\ mol^{-1}$$

$$k \propto \exp(\frac{-\Delta G^{\ddagger}}{RT})$$

5.4 Calculation for the alternative mechanism of thiol addition

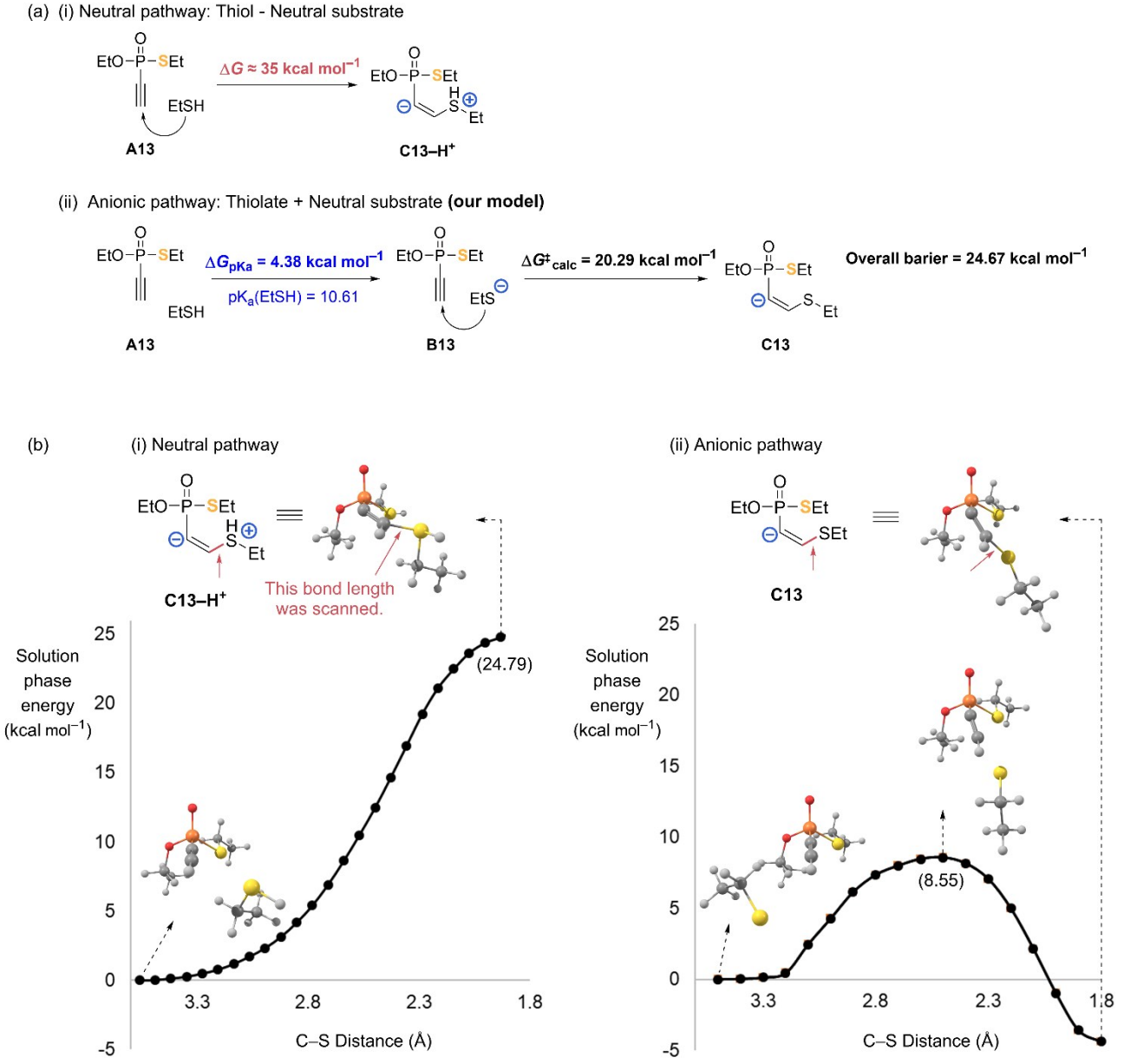

Fig. S5 (a) Two possible mechanisms were considered as the models for the nucleophilic attack. (b) Solution phase energy and structures calculated along the C–S distance.

Two possible mechanisms are depicted in Fig. S5a, which differ in the sequence of deprotonation events along the reaction pathway: (i) Neutral pathway, where EtSH attacks the electrophile forming a zwitterionic intermediate **C13–H**$^+$, and (ii) Anionic pathway where EtSH is first deprotonated to EtS$^-$ and attacks the electrophile to generate **C13**.

Another possibility of protonated electrophile participating in the reaction was ruled out due to the low basicity of **13**. The pKa of the protonated phosphoryl (P=OH$^+$) group of **13** was calculated using DFT with the reference pKa value (–3.6) of trimethylphosphate[26] following the reported protocol.[27] Based on the calculated pKa value of –4.51, the protonation of **13** is considered very unlikely in the reaction condition.

The relative free energy of **C13–H⁺** was estimated based on the scan calculations as plotted in Fig. S5b. The free energy along the C–S bond scan was calculated with the double-ζ quality basis set, following the same protocol as the geometry optimizations. 'Solution phase energy' refers to the sum of electronic energy and solvation energy, which needs additional zero-point energy and entropy contributions to arrive at the solution phase Gibbs free energy. For **C13–H⁺** in (i) Neutral pathway, for instance, its formation was found to be 24.8 kcal mol^{-1} uphill relative to the reactants (**A13**). The electronic energy at the triplet-ζ basis set shows a similar value: 23.5 kcal mol^{-1} uphill from the reactants. As the entropic penalty for bimolecular reactions is considered to be ca. 11 kcal mol^{-1},[28] the formation of **C13–H⁺** can be assumed to require the free energy of ~34.5 kcal mol^{-1}.

The transition state for (ii) Anionic pathway, on the other hand, was properly located with the step barrier of 20.3 kcal mol^{-1}. Considering ΔG_{pKa} of 4.4 kcal mol^{-1}, the overall barrier is 24.7 kcal mol^{-1}. Based on this comparison, we considered the anionic pathway as the viable model of the reaction.

5.5 Second-order perturbation analysis

The amount of all possible hyperconjugation interactions was analyzed with the second-order perturbation energy. The major difference arises from LP(C)→σ*(P–X) interaction as highlighted in red in Fig. S6; 22.2 (X = S), 18.9 (X = O), and 11.6 (X = NH) kcal mol^{-1}. This result demonstrates that the effect of heteroatom X is a major factor to determine the total amount of hyperconjugation which is stabilizing the electron density of the carbanion lone pair.

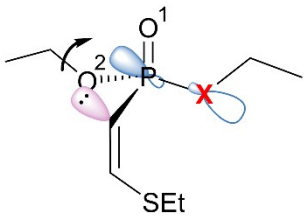

X = S (**C13**)		X = O (**C14**)		X = NH (**C15**)	
LP(C) → σ*(P–S)	22.18	LP(C) → σ*(P–O)	18.85	LP(C) → σ*(P–N)	11.56
LP(C) → σ*(P–O^2)	11.13	LP(C) → σ*(P–O^2)	6.82	LP(C) → σ*(P–O^2)	8.27
LP(C) → σ*(P–O^1)	0.65	LP(C) → σ*(P–O^1)	<0.5	LP(C) → σ*(P–O^1)	1.89
LP(C) → σ*(C–S)	32.83	LP(C) → σ*(C–S)	35.47	LP(C) → σ*(C–S)	36.08
LP(C) → σ*(C–H)	4.44	LP(C) → σ*(C–H)	4.45	LP(C) → σ*(C–H)	3.83
LP(C) → σ*(O^2–C)	0.90	LP(C) → σ*(O^2–C)	0.75	LP(C) → σ*(O^2–C)	0.88
(remote hyperconjugation)		(remote hyperconjugation)		(remote hyperconjugation)	
Total	72.13	Total	66.84	Total	62.51

Fig. S6 Second-order perturbation energies of carbanion intermediates **C13**–**C15**. Interaction energies are in kcal mol^{-1}.

The LP(S)→π*(C≡C) donor-acceptor interactions were analyzed for two isomeric structures **B-TS13** and **B-TS13-*E***. The energy is related to the effectiveness of the C–S bond-forming interaction in the transition states. As shown in Fig. S7, **B-TS13** features the interaction of 83.9 kcal mol^{-1}, whereas the interaction is significantly reduced to 73.7 kcal mol^{-1} for **B-TS13-*E***. The analysis demonstrates that the LP(S)→π*(C≡C) interaction is stronger in the *Z*-conformation.

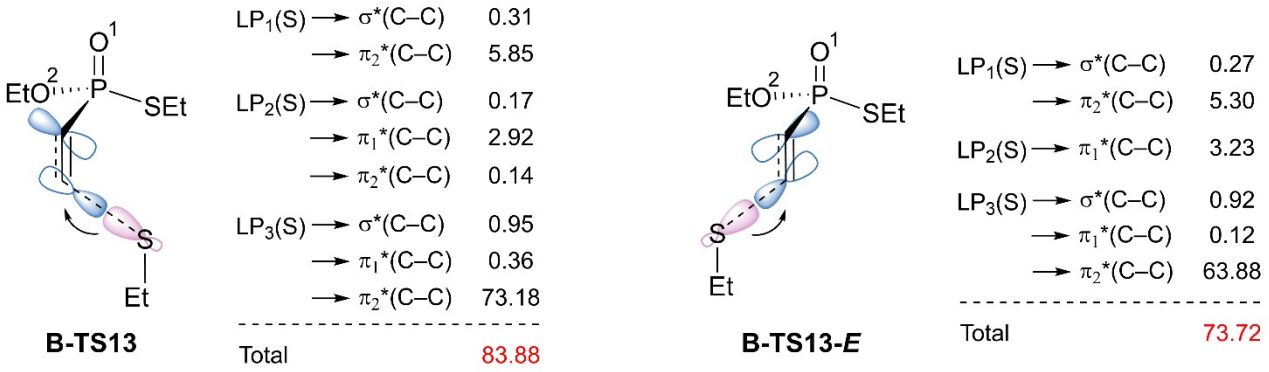

Fig. S7 Second-order perturbation energies of transition states **B-TS13** and **B-TS13-*E***. Interaction energies are in kcal mol^{-1}.

5.6 Steric exchange energy analysis

In order to consider the repulsive term of interaction energy and fully account for the relative stability of the carbanion intermediates **C13–C15**, we performed the steric energy calculation using NBO software. We evaluated the change in steric energies compared to the reference geometry where the two reactants are at a distance of 8 Å, following the recommendation in the NBO manual. The geometry was treated as two separate molecular segments for constructing the NBOs, by specifying 'unit 1' as the electrophile fragment and 'unit 2' as the thiolate fragment using 'MOLUNIT' keyword. Therefore, even in the intermediate C geometry, the π(C≡C) and LP$_3$(S) orbitals are constructed as NBOs instead of the σ(C–S) orbital. As for 'ΔEsteric, pair', we refer to the change in the total amount of pairwise steric exchange interactions between two occupied orbitals that do not share any atoms (i.e. "disjoint" pairs).

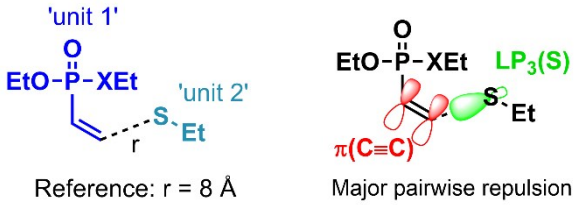

Fig. S8 Molecular units designated for steric energy calculation.

As summarized in Table S1, while the bond is longer in the order of **C13** (1.823 Å) < **C14** (1.830 Å) < **C15** (1.841 Å), there was larger steric repulsion in the order of **C13** (136.2 kcal mol^{-1}) < **C14** (146.5 kcal mol^{-1}) < **C15** (151.3 kcal mol^{-1}).

Table S1. Comparison of interaction energies (in kcal mol^{-1}) of intermediates C13–C15.

	ΔE(SCF)	ΔEdistortion	ΔEinteraction[a]	ΔEsteric, pair[b]	C–S distance (Å)
C13 (X = S)	–27.10	50.30	–77.39	136.22	1.823
C14 (X = O)	–25.83	48.68	–74.51	146.5	1.830
C15 (X = NH)	–23.57	46.95	–70.52	151.28	1.841

[a]ΔEinteraction = ΔE(SCF) – ΔEdistortion.
[b]NBO-calculated energy, relative to the reference geometry where the electrophile and thiolate are at a distance of 8 Å.

We investigated the most representative components of the steric energy change in **C13–C15** as tabulated below (Table S2). The steric repulsion of π(C≡C) orbital contributes to the general trend. Among the interactions of π(C≡C) orbital, repulsion with LP(S) orbital was governing the trend; **13** (54.7 kcal mol–1) < **14** (58.2 kcal mol–1) < **15** (60.0 kcal mol–1). The trend in repulsion is well understood considering the NBO-calculated occupancy. The occupancy on the π(C≡C) and LP_3(S) orbital indicates there is more electron density on the C–S moiety in the order of **13** < **14** < **15**, while the occupancy of σ*(P–X) orbital shows there is less density in the same order. Taken together, the steric energies and occupancy provide the clue on how π-bonding electrons (which formally turns into the carbanion lone pair) are delocalized throughout the molecule as a response to the bond formation with the thiolate. The electron density of **C13** most effectively spread out to the σ*(P–S) orbital *via* hyperconjugation, and **C13** possesses the least repulsion between the π-electrons and the LP(S), and despite the shortest C–S bond.

For other pairwise steric interactions such as π(C≡C)- σ(P–X), LP3(S)- σ(C–H), and LP_3(S)-LP(X), we did not see a significant difference among different substrates.

Table S2. Steric energy analysis for the intermediates 13C, 14C, and 15C.

	Representative orbitals			Representative pairwise interaction	NBO-calculated occupancy		
	π(C≡C)	LP_3(S)	σ(P–X)	LP3(S)- π(C≡C)	π(C≡C)	LP_3(S)	σ*(P–X)
C13 (X = S)	65.92	31.31	2.17	54.75	1.82	1.07	0.284
C14 (X = O)	73.08	29.98	–0.75	58.18	1.86	1.09	0.219
C15 (X = NH)	73.38	32.26	1.04	60	1.87	1.11	0.182

In conclusion, the trend in repulsive steric energy between two molecular segments supports the reactivity, together with the strength of the attractive interaction. Both energy terms can be interpreted as a result of electronic delocalization. Specifically, for **13** (X = S) there is the most effective electronic dissipation to the σ*(P–

X) orbital compared to other electrophiles, so that it lowers the repulsive interaction between the existing and incoming electron densities and enables the most effective bond-forming interaction.

5.7 Analysis on E/Z-selectivity

In order to elucidate the stereoselectivity in more detail, we performed an energy decomposition for the two reaction pathways of **13** that yield the intermediates in *Z*- and *E*-conformation. As depicted in Fig. S9, *E*-pathway is higher in energy until the two reactants reach a distance less than 2.0 Å. At a bond distance further than 2.4 Å, there is insufficient bond-forming interaction; and at a shorter distance, there is greater distortion energy.

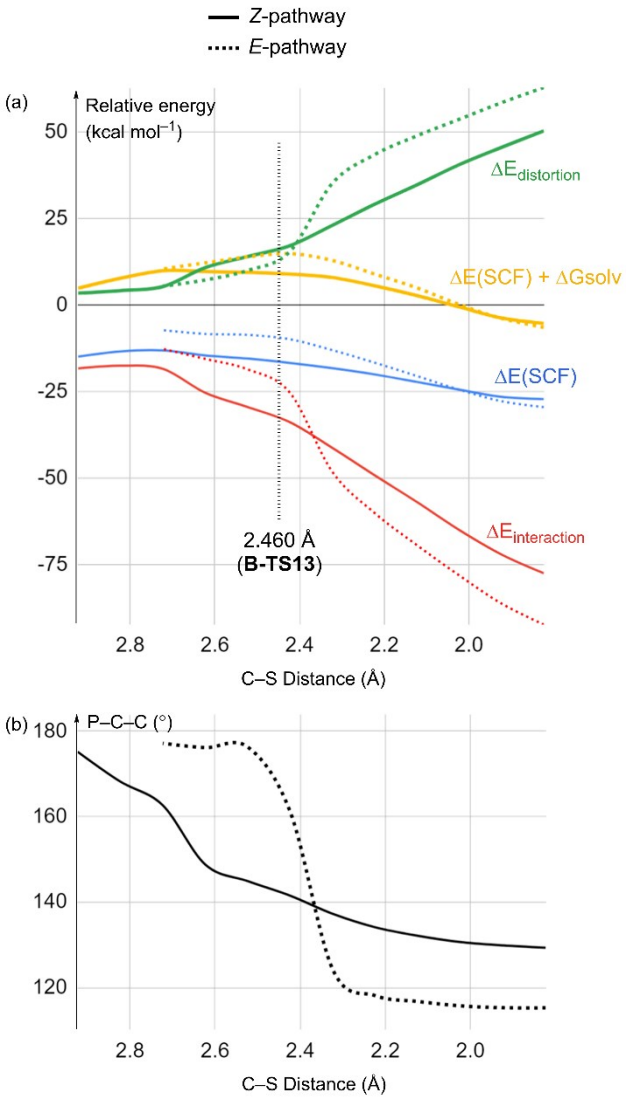

Fig. S9. Change in energies (top) and P–C–C bond angle (bottom) along the reaction coordinate of **13** in *Z*- and *E*-conformation. Geometries of each point, at intervals of 0.5 Å, were obtained with relaxed scan calculations starting from **C13** and **C13-*E***, respectively.

The low interaction energy in the *E*-pathway, before reaching 2.4 Å, means that the bond-forming interaction is relatively unfavorable due to the stereochemistry. As summarized in Table S3, the second-order perturbation energy of $LP_3(S)\rightarrow\pi^*(C\equiv C)$ well represents the weaker attractive interaction in the *E*-conformers (at 2.523 and 2.460 Å). The repulsive interaction is also weaker for *E*-conformers.

Since the transition state optimization in the *E*-conformer converges to *Z*-conformation, the estimated transition state **B-TS13-*E*** was obtained from the transition state calculation with the constrained P–C–C–S group, using the same bond distances as **B-TS13**, yet modifying the dihedral angle to 180°.

Once the reactants get closer than 2.4 Å, the E-pathway features an abrupt increase in distortion energy, which mainly comes from the decrease of P–C–C angle. The smaller P–C–C angle of the E-conformers indicates the sp^2-hybridized lone pair has more s-character and more centered on the carbon atom. Because the C–S bond is synperiplanar to the lone pair orbital in *E*-conformers, the charge is less effectively delocalized through the hyperconjugation $LP_3(S)\rightarrow\sigma^*(C–S)$. The excessive electron density localized on the carbanion center gives rise to the higher barrier.
This gigantic distortion energy is finally overcome with the strong bonding interaction at the distance of 2.0 Å. At the stationary point, **C13-*E*** has a much stronger C–S bond with a shorter bond length of 1.794 Å with less steric repulsion, thus is thermodynamically more stable.

Table S3. Analysis of interaction energies (in kcal mol^{-1}) for the reaction of 13 in *Z*- and *E*-conformation.

C–S distance (Å)	Stereochemistry	ΔE(SCF)	Δdistortion	Δinteraction	Δsecond-order perturbation $LP_3(S)\rightarrow\pi^*(C\equiv C)$	Δsteric, pair
2.523	Z	–15.47	14.00	–29.47	62.06	56.62
	E	–8.62	9.96	-18.59	48.35	46.23
2.460	Z (**B-TS13**)	–15.47	11.39	–26.87	69.34	70.21
	E (**B-TS13-*E***)[a]	–10.15	14.83	–24.97	59.08	67.68
1.823	Z (**C13**)	–27.19	50.32	–77.51	-[b]	136.22
1.794	E (**C13-*E***)	–29.43	64.15	–93.58	-[c]	93.52

[a]Transition state calculation was done with the constrained geometry of P–C–C–S group.
[b]$LP_3(S)\rightarrow\pi^*(C\equiv C)$ interaction is severely overestimated in this geometry.
[c]$\pi^*(C\equiv C)$ orbital is not constructed in this geometry.

Although *E*-pathway is thermodynamically more stable at the final stage of the reaction attributed to the stronger C–S bond, the intermediary structures demand substantial energetic cost because of the lack of stabilization by means of hyperconjugation to the $\sigma^*(C–S)$ orbital. As a result, the formation of the *E*-product is hindered by the higher activation energy.

5.8 Molecular orbital analysis

For the ethynyl P(V) electrophiles, **13**–**15**, the molecular orbital analysis was conducted (Fig. S10a). MO analysis was performed using Amsterdam Density Functional (ADF) 2019 suite of programs,[29].[30] employing M06-2X functional and TZ2P basis set.[31] In particular, the MO with the π^*(C≡C) orbital as the major component was analyzed for comparison as it represents the acceptor orbital for the reaction. Even though π^*(C≡C) orbital is expected to be the LUMO of the electrophiles, which was true for **13** and **14**, it was not the case for **15**. The LUMO+2 of **15** was found as π^*(C≡C) orbital. The orbital energies were calculated in the order of 0.00 (**13**) < 0.45 (**14**) < 0.54 (**15**, LUMO) < 0.82 eV (**15**, LUMO+2), indicating that **13** has the lowest LUMO that is favorable for the nucleophilic addition. In order to find out the difference of the pertaining orbitals, the percentage contributions of the orbitals from the ethynyl group (C≡C), phosphorus atom (P), and heteroatoms (X) were compared. The percentage contribution was calculated as implemented in ADF, which is based on Mulliken population analysis of the fragment orbitals. The contribution from the P–X moiety was much greater in **13** (P: 24 % and S: 19 %) than in the case of **14** and **15**. Therefore, we assumed that the P–S bond is responsible for lowering the LUMO of **13**. As shown in Fig. S10b, the LUMO of **13** can be understood as the result of an in-phase combination of π^*(C≡C) and σ^*(P–S) orbital. We imagined that σ^*(P–X) orbitals for X = O and NH are much higher in energy and thus does not effectively mix into the π^*(C≡C) orbital.

(a)

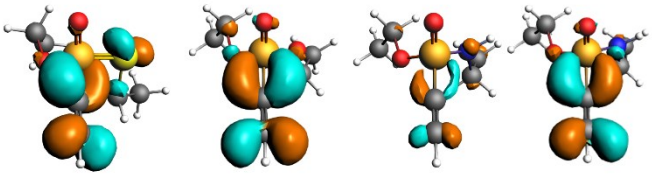

Orbital		**13** (X = S) LUMO	**14** (X = O) LUMO	**15** (X = NH) LUMO	LUMO+2[a]
Orbital energy (eV)		–0.002	0.446	0.539	0.824
Contribution (%)	C≡C[b]	57 %	79 %	17 %	73 %
	P	**24 %**	13 %	10 %	13 %
	X	**19 %**	2 %	2 %	4 %

Significant mixing from P–S moiety

(b)

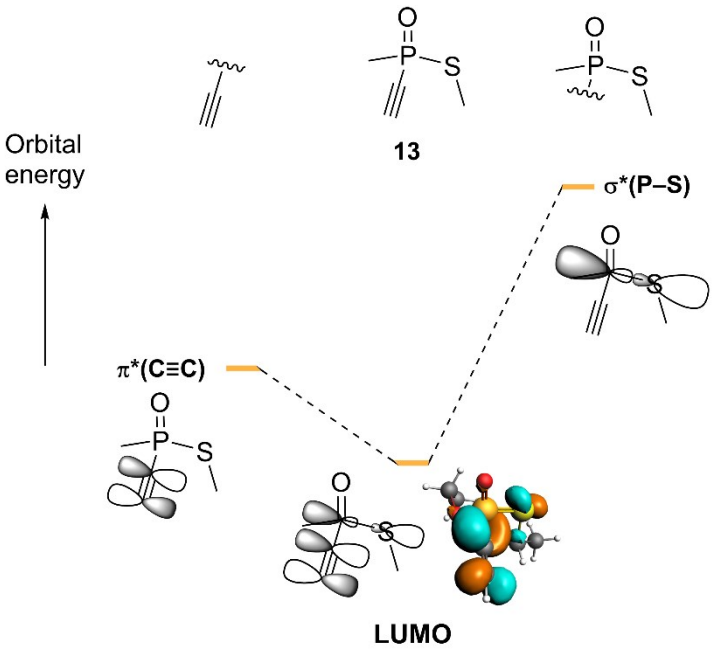

Fig. S10 (a) Molecular orbitals of **13**–**15** that are subjected to the HOMO-LUMO interaction for the nucleophilic thiol addition. [a]For **15**, the LUMO+2 was found to have larger π*(C≡C) character than the LUMO. [b]For C≡C contributions, the percentage contribution from the two related carbon atoms were added up. (b) The conceptual in-phase combination between π*(C≡C) and σ*(P–S) that lowers the LUMO of **13**. (Isodensity value = 0.05 a.u.)

6. References

[1] B. E. M. El-Gendy, E. H. G. Zadeh, A. C. Sotuyo, G. G. Pillai and A. R. Katritzky, *Chem Biol Drug Des*, 2013, **81**, 577–582.

[2] U.S. Pat., US-5994340-A, November 30, 1999.

[3] A. L. Baumann, S. Schwagerus, K. Broi, K. Kemnitz-Hassanin, C. E. Stieger, N. Trieloff, P. Schmieder and C. P. R. Hackenberger, *J. Am. Chem. Soc.*, 2020, **142**, 9544–9552.

[4] M. A. Kasper, M. Glanz, A. Stengl, M. Penkert, S. Klenk, T. Sauer, D. Schumacher, J. Helma, E. Krause, M. C. Cardoso, H. Leonhardt and C. P. R. Hackenberger, *Angew. Chem. Int. Ed.*, 2019, **58**, 11625–11630.

[5] M. Mikolajczyk, B. Costisella and S. Grzejszczak, *Tetrahedron*, 1983, **39**, 1189–1193.

[6] R. Dennington, T. A. Keith, and J. M. Millam, GaussView (Version 6.1), Semichem Inc., Shawnee Mission, KS, 2016.

[7] R. G. Parr, W. Yang, *Density Functional Theory of Atoms and Molecules*, Oxford University Press, New York, **1989**.

[8] M. J. Frisch, G. W. Trucks, H. B. Schlegel, G. E. Scuseria, M. A. Robb, J. R. Cheeseman, G. Scalmani, V. Barone, G. A. Petersson, H. Nakatsuji, X. Li, M. Caricato, A. V. Marenich, J. Bloino, B. G. Janesko, R. Gomperts, B. Mennucci, H. P. Hratchian, J. V. Ortiz, A. F. Izmaylov, J. L. Sonnenberg, D. Williams-Young, F. Ding, F. Lipparini, F. Egidi, J. Goings, B. Peng, A. Petrone, T. Henderson, D. Ranasinghe, V. G. Zakrzewski, J. Gao, N. Rega, G. Zheng, W. Liang, M. Hada, M. Ehara, K. Toyota, R. Fukuda, J. Hasegawa, M. Ishida, T. Nakajima, Y. Honda, O. Kitao, H. Nakai, T. Vreven, K. Throssell, J. A. Montgomery, Jr., J. E. Peralta, F. Ogliaro, M. J. Bearpark, J. J. Heyd, E. N. Brothers, K. N. Kudin, V. N. Staroverov, T. A. Keith, R. Kobayashi, J. Normand, K. Raghavachari, A. P. Rendell, J. C. Burant, S. S. Iyengar, J. Tomasi, M. Cossi, J. M. Millam, M. Klene, C. Adamo, R. Cammi, J. W. Ochterski, R. L. Martin, K. Morokuma, O. Farkas, J. B. Foresman, and D. J. Fox, Gaussian 16 (Revision A.03), Gaussian, Inc., Wallingford CT, 2016.

[9] Slater, J. C. *Quantum Theory of Molecules and Solids, Vol. 4: The Self-Consistent Field for Molecules and Solids,* McGraw-Hill, New York, 1974.

[10] S. H. Vosko, L. Wilk and M. Nusair, *Can. J. Phys.*, 1980, **58**, 1200–1211.

[11] A. D. Becke, *Phys. Rev. A.*, 1988, **38**, 3098–3100.

[12] C. T. Lee, W. T. Yang and R. G. Parr, *Phys. Rev. B.*, 1988, **37**, 785–789.

[13] K. Raghavachari, *Theor. Chem. Acc.*, 2000, **103**, 361–363.

[14] R. A. Kendall, T. H. Dunning and R. J. Harrison, *J. Chem. Phys.*, 1992, **96**, 6796–6806.

[15] D. E. Woon and T. H. Dunning, *J. Chem. Phys.*, 1993, **98**, 1358–1371.

[16] G. Scalmani and M. J. Frisch, *J. Chem. Phys.*, 2010, **132**.

[17] A. D. Bochevarov, E. Harder, T. F. Hughes, J. R. Greenwood, D. A. Braden, D. M. Philipp, D. Rinaldo, M. D. Halls, J. Zhang and R. A. Friesner, *Int. J. Quantum. Chem.*, 2013, **113**, 2110–2142.

[18] Y. Zhao and D. G. Truhlar, *Theor. Chem. Acc.*, 2008, **120**, 215–241.

[19] R. Ditchfield, W. J. Hehre and J. A. Pople, *J. Chem. Phys.*, 1971, **54**, 724-728.

[20] B. Marten, K. Kim, C. Cortis, R. A. Friesner, R. B. Murphy, M. N. Ringnalda, D. Sitkoff and B. Honig, *J. Phys. Chem.*, 1996, **100**, 11775–11788.

[21] S. R. Edinger, C. Cortis, P. S. Shenkin and R. A. Friesner, *J. Phys. Chem. B*, 1997, **101**, 1190–1197.

[22] M. Friedrichs, R. H. Zhou, S. R. Edinger and R. A. Friesner, *J. Phys. Chem. B*, 1999, **103**, 3057–3061.

[23] A. A. Rashin and B. Honig, *J. Phys. Chem.*, 1985, **89**, 5588–5593.

[24] T. H. Dunning, *J. Chem. Phys.*, 1989, **90**, 1007–1023.

[25] E. P. Serjeant, B. Dempsey B, International Union of Pure and Applied Chemistry (IUPAC). *Ionisation Constants of Organic Acids in Aqueous Solution, IUPAC Chemical Data Series No. 23,* Oxford, New York: Pergamon Press, 1979.

[26] L. Azema, S. Ladame, C. Lapeyre, A. Zwick and F. Lakhdar-Ghazal, *Spectrochim. Acta A*, 2005, **62**, 287–292.

[27] J. F. Huo and J. B. Wang, *Chinese J. Org. Chem.*, 2020, **40**, 239–240.

[28] H. Ryu, J. Park, H. K. Kim, J. Y. Park, S. T. Kim and M. H. Baik, *Organometallics*, 2018, **37**, 3228–3239.

[29] G. te Velde, F. M. Bickelhaupt, E. J. Baerends, C. F. Guerra, S. J. A. Van Gisbergen, J. G. Snijders and T. Ziegler, *J. Comput. Chem.*, 2001, **22**, 931–967.

[30] C. F. Guerra, J. G. Snijders, G. te Velde and E. J. Baerends, *Theor. Chem. Acc.*, 1998, **99**, 391–403.

[31] E. Van Lenthe and E. J. Baerends, *J. Comput. Chem.*, 2003, **24**, 1142–1156.

7. Appendix

7.1 DFT-calculated energy components and coordinates

Table S4. Computed energy components for optimized structures

	E(SCF)/(eV)	ZPE/(kcal mol^{-1})	S(gas)/(cal mol^{-1}·K)	G(solv)/(kcal mol^{-1})
	M06-2X/cc-pVTZ(-f)	M06-2X/6-31G(d,p)	M06-2X/6-31G(d,p)	M06-2X/6-31G(d,p)
EtSH	-13006.857	47.606	68.013	-4.01
EtS^-	-12991.132	41.275	65.978	-78.31
10	-30652.625	119.356	116.359	-11.36
B-TS10	-43644.277	160.977	147.303	-65.51
C10	-43644.449	161.556	146.12	-65.95
D10	-43660.547	170.93	143.338	-13.97
13	-30618.531	104.527	112.275	-13.6
B-TS13	-43610.383	146.201	146.33	-64.93
C13	-43610.887	147.153	143.164	-68.09
D13	-43626.984	156.039	139.133	-16.61
B-TS13-*E*	-43610.152	146.049	140.915	-65.2
C13-*E*	-43610.988	147.276	143.025	-66.98
D13-*E*	-43627.043	156.072	139.471	-16.7
14	-21830.451	106.52	109.724	-15.3
BTS-14	-34822.316	148.57	135.978	-66.82
C14	-34822.703	149.336	135.909	-70.61
D14	-34839.059	158.298	132.735	-17.08
15	-21289.51	114.243	110.044	-16.59
BTS-15	-34281.285	156.154	137.009	-66.52
C15	-34281.664	157.187	133.188	-70.17
D15	-34297.891	165.721	134.987	-19.78

Table S5. **Cartesian coordinates of the optimized geometries**

The cartesian coordinates of optimized geometries are given below in the standard XYZ format, and units are in Å.

```
================================
EtSH
================================
  S  -0.522487998  -0.095818713  -1.357048035
  H  -0.525959492   1.219089985  -1.656197429
  C  -0.521623611   0.082114160   0.485213935
  H   0.365029663   0.644266605   0.791731119
  H  -1.408607721   0.643199384   0.792765260
  C  -0.520859838  -1.305560350   1.127724528
  H   0.365473896  -1.876943588   0.835180998
  H  -1.407866716  -1.877012491   0.837007344
  H  -0.519810736  -1.212433815   2.218603849

================================
EtS⁻
================================
  S  -0.522077262  -0.012091191  -1.336641192
  C  -0.521582544   0.005197069   0.491481721
  H   0.356485933   0.545746386   0.876609325
  H  -1.399191260   0.546133995   0.877143562
  C  -0.521561265  -1.395468950   1.105756521
  H   0.358575225  -1.949159265   0.763300896
  H  -1.401169658  -1.949404120   0.762421310
  H  -0.522039533  -1.384233356   2.209656954
================================
10
================================


  O   2.059196699   1.142986628   4.459522335
  P   0.726460934   0.471360258   4.425354865
  O   0.128662343   0.102754745   2.985205753
  S   0.725183800  -1.398169304   5.369368147
  C  -0.615754846   1.414109352   5.138159326
  C   0.873047784  -0.723537648   2.045887085
  H   1.100901136  -0.087044805   1.188437471
  H   1.816790770  -1.043482264   2.498886440
  C   0.013910051  -1.907384118   1.656974830
  H  -0.186183201  -2.546989783   2.521708652
  H  -0.939153266  -1.568047572   1.242740864
  H   0.529545928  -2.502493166   0.898088553
  C   1.567466903  -0.957586754   6.947174040
  H   2.583452551  -0.638051451   6.710594911
  H   1.027198986  -0.122791469   7.401643648
  C   1.555978674  -2.178389941   7.858312636
  H   0.533647447  -2.489261371   8.090292651
  H   2.080592285  -3.021203979   7.399661251
  H   2.059549107  -1.933910344   8.797236404
  C  -0.360333670   2.507729002   5.857216346
  H  -1.621627890   1.019291449   4.999026209
  H   0.656199100   2.871612618   5.991476755
  H  -1.160067373   3.074431228   6.328314519
================================
B-TS10
================================
  P   1.194887098  -0.166591754   0.191055209
  O   2.365544083  -0.793638821   0.899897790
  O   1.584601318   0.573832426  -1.199691214
  C   1.992790214  -0.151001112  -2.369530070
  H   2.924184305  -0.688781666  -2.157048661
  H   1.216703514  -0.879722697  -2.629026415
  C   2.172153073   0.849620706  -3.492040661
  H   1.229343698   1.368572133  -3.687328030
  H   2.935001646   1.589372161  -3.235435886
  H   2.479398535   0.331191056  -4.404224159
  S  -0.139998214  -1.731337913  -0.405786598
  C   0.970258982  -3.168611273  -0.689282826
  H   1.652713387  -2.938482664  -1.511342960
  H   1.563565945  -3.320114303   0.214127817
  C   0.120938806  -4.391363865  -1.018922144
  H  -0.567423819  -4.625313110  -0.201938742
  H  -0.468114257  -4.231602391  -1.926858748
  H   0.765840621  -5.259365518  -1.180860955
  C   0.260656170   1.025293887   1.006707797
  C  -0.566305646   1.908823101   0.288057100
  H  -0.234398544   2.222590763  -0.696440809
  S  -2.522122144   1.086518156  -0.483435483
  C  -3.414326007   2.685319719  -0.612249556
  H  -2.739590488   3.416739006  -1.071312583
  H  -3.643667825   3.053596901   0.393165968
  C  -4.698101561   2.581959402  -1.430717790
  H  -4.489485552   2.242984312  -2.449730928
  H  -5.399141209   1.874116456  -0.978418004
  H  -5.195270833   3.556024796  -1.491346169
  H  -1.056589619   2.703492778   0.847227083
  H   0.051312858   0.807505717   2.052241577
================================
C10
================================
  P   1.024802148  -0.224404528   0.138714782
  O   2.145054998  -0.955726667   0.840574673
  O   1.475248930   0.455153144  -1.276541571
  C   1.847547188  -0.317021609  -2.421565083
  H   2.710889444  -0.947401264  -2.174829173
  H   1.013323238  -0.966981510  -2.709277666
  C   2.174035221   0.646813189  -3.543935085
  H   1.300674445   1.262458649  -3.777922893
  H   3.001608525   1.303633010  -3.263600164
  H   2.456767048   0.089531090  -4.441063159
  S  -0.346451888  -1.790904714  -0.520191965
  C   0.694409376  -3.261405836  -0.880645524
  H   1.445209356  -2.994980792  -1.628389095
  H   1.218012272  -3.546068409   0.033772399
  C  -0.190218791  -4.394130677  -1.392665723
  H  -0.952863746  -4.665921172  -0.656735009
  H  -0.698691438  -4.109233167  -2.318757383
  H   0.415791488  -5.281680963  -1.596860935
  C   0.220434242   1.035497463   0.928404516
  C  -0.675537141   1.971945838   0.196434831
  H  -0.263793395   2.254708964  -0.774572163
  S  -2.394506801   1.279507623  -0.167633819
  C  -3.275918710   2.755393923  -0.796095532
  H  -2.713099564   3.166661404  -1.639717775
  H  -3.300289486   3.515607675  -0.009042294
```

C	-4.692400383	2.385596320	-1.228457051
H	-4.681077564	1.643597300	-2.031794329
H	-5.268040820	1.973327480	-0.394645239
H	-5.219967909	3.270436414	-1.595080642
H	-0.868182676	2.888976693	0.762859582
H	-0.031925957	0.808366615	1.964045573

==========

D10

==========

P	0.782357642	-0.444177746	-0.015692785
O	2.005719932	-1.113139516	0.526730670
O	1.018748973	0.500284795	-1.292634694
C	1.579415735	-0.046803358	-2.509795109
H	2.653159448	-0.194130572	-2.361815049
H	1.112163755	-1.017806089	-2.713121331
C	1.283933094	0.931363789	-3.626307295
H	0.203885744	1.050317346	-3.748386519
H	1.724152464	1.908762172	-3.411904280
H	1.702723746	0.558394488	-4.564870499
S	-0.653306056	-1.862483174	-0.614342020
C	0.336566448	-3.415971990	-0.568810112
H	1.228822902	-3.281138811	-1.182712226
H	0.645317733	-3.599762047	0.460869778
C	-0.539229117	-4.541849630	-1.106744515
H	-1.442429133	-4.669150346	-0.502882426
H	-0.837886712	-4.350716291	-2.141231521
H	0.021009156	-5.480063319	-1.081059704
C	-0.009585310	0.726142852	1.128291532
C	-0.899916359	1.806862868	0.509503368
H	-0.344765650	2.358270690	-0.253249114
S	-2.402934320	1.105916401	-0.252721079
C	-3.171994937	2.633639779	-0.896710000
H	-2.473174524	3.110945068	-1.589470888
H	-3.345576526	3.314482993	-0.058177941
C	-4.482816901	2.290736112	-1.598103238
H	-4.317580152	1.617512903	-2.444106795
H	-5.188981098	1.814729851	-0.911612798
H	-4.947430632	3.203679669	-1.979773424
H	0.829752259	1.211949301	1.642053727
H	-1.201557252	2.505168707	1.296019922
H	-0.543077145	0.133977528	1.880344569

==========

13

==========

P	3.875669873	-0.219701191	4.834496974
O	3.826300514	-0.024281338	3.359611966
O	2.788705600	-1.210783650	5.457540378
C	2.646763783	-2.557337720	4.908181876
H	1.585226687	-2.668018786	4.678624318
H	3.209741420	-2.635301056	3.972496900
C	3.111934669	-3.571378699	5.931807743
H	4.188611556	-3.485566134	6.106606887
H	2.583985794	-3.431928943	6.879054650
H	2.903308754	-4.580490007	5.565319621
S	5.750275950	-0.918682640	5.377830746
C	5.610911509	-1.025584826	7.210577056
H	5.641525499	-0.010166038	7.610521655
H	4.648210029	-1.478795356	7.461037323
C	6.774238922	-1.865044065	7.725913965
H	6.724683903	-2.888322754	7.343303193
H	7.735720446	-1.431552964	7.435357804
H	6.735777243	-1.902142541	8.817373655
C	3.565750409	1.222686591	5.795320526
C	3.434004899	2.242162471	6.434069927
H	3.303298229	3.151840328	6.995453753

==========

B-TS13

==========

P	1.037589926	0.679207611	-1.365470618
O	1.133602609	1.225386966	-2.755451315
O	0.374414160	-0.780729795	-1.211987026
C	0.864391642	-1.903174887	-1.984571542
H	0.100538490	-2.134570757	-2.730796137
H	1.783521908	-1.621869708	-2.507294154
C	1.104698975	-3.064102445	-1.043221304
H	1.888741427	-2.815853525	-0.322218943
H	0.191082044	-3.310319483	-0.495895063
H	1.418138530	-3.944998676	-1.609545195
S	2.955022856	0.306309353	-0.570872827
C	3.899296681	1.693275421	-1.315667560
H	4.943596881	1.374786098	-1.265653382
H	3.611828534	1.748763985	-2.366756604
C	3.684247608	3.014139425	-0.594514995
H	2.627289441	3.298131519	-0.594602878
H	4.009067474	2.950011757	0.447056527
H	4.257355459	3.804058716	-1.089348622
C	0.048190684	1.581343577	-0.280369296
C	-0.095417785	2.230515350	0.771101812
H	-0.768570367	2.763523944	1.423406906
S	1.679997324	2.765238844	2.388341957
C	0.463124154	3.124361916	3.710225604
H	-0.436751520	3.565576995	3.257205253
H	0.867077132	3.897715343	4.370570125
C	0.064425119	1.898543638	4.524923449
H	-0.373668466	1.132147003	3.878181567
H	0.935821947	1.459892329	5.019667836
H	-0.670647699	2.159445472	5.294416548

==========

C13

==========

P	0.895708000	-0.310788654	0.028991211
O	2.396479084	-0.337673126	0.135958294
O	0.503904987	0.924498708	-0.969861595
C	-0.886827180	1.144658087	-1.279130142
H	-1.511396437	0.435546541	-0.724100289
H	-1.139562201	2.151096580	-0.933501933
C	-1.116638581	1.001609405	-2.770934034
H	-0.465940789	1.680002077	-3.329693124
H	-0.920677963	-0.025826477	-3.092337693
H	-2.156510149	1.244758237	-3.009243956
S	0.291067188	-2.015118677	-1.159738522
C	1.471276983	-1.890332217	-2.561783555
H	1.447398572	-0.861669657	-2.931330176
H	2.476098384	-2.097103321	-2.189276857
C	1.065158536	-2.873211098	-3.654130910
H	1.066365004	-3.902492962	-3.283187370
H	0.063999717	-2.649059824	-4.034272406
H	1.767903251	-2.814309737	-4.489999569
C	0.008913083	-0.076547280	1.487292376
C	-1.128484886	-0.645543881	1.883821062
H	-1.615631257	-0.373471095	2.826415671
S	-2.158751062	-1.912540005	1.073203244
C	-3.520773912	-2.106460381	2.283245227
H	-3.976699521	-1.127747649	2.457126121
H	-3.107005616	-2.467225951	3.228828632
C	-4.551478709	-3.089395693	1.735109243
H	-4.981047544	-2.733159729	0.794039904
H	-4.109501198	-4.074519739	1.557862698

H	-5.367157843	-3.211283993	2.453218986

==========

D13

==========

P	0.905046255	-0.405120214	-0.040325542
O	2.375191005	-0.311372772	0.209969644
O	0.509793402	0.675257574	-1.169337710
C	-0.858759658	0.879167620	-1.588873832
H	-1.294531668	-0.085420745	-1.873051114
H	-1.426720831	1.284532276	-0.744673181
C	-0.840430910	1.835444738	-2.761003703
H	-0.397365788	2.791949496	-2.472189754
H	-0.264489030	1.414213982	-3.589818705
H	-1.864006351	2.011872529	-3.101837925
S	0.279255295	-2.251565570	-0.798214582
C	1.331310955	-2.297287337	-2.314935557
H	1.103730883	-1.410780135	-2.911356257
H	2.376138973	-2.256374453	-2.002037235
C	1.025704415	-3.576305995	-3.083568329
H	1.233813622	-4.463543497	-2.479151590
H	-0.019308694	-3.607301647	-3.403495755
H	1.657500388	-3.616625671	-3.974783634
C	-0.056344306	-0.089491719	1.434898664
C	-1.335227252	-0.356007754	1.756299441
H	-1.682534202	-0.035475418	2.739570129
S	-2.563818542	-1.177499401	0.821492815
C	-4.010658505	-1.017248691	1.936957564
H	-4.165299665	0.042873578	2.150877388
H	-3.788288205	-1.543699607	2.868148094
C	-5.223667902	-1.620907153	1.236636595
H	-5.444654556	-1.098394259	0.301288391
H	-5.070211811	-2.680763922	1.013103778
H	-6.098448694	-1.535433040	1.886302050
H	0.545615336	0.423200097	2.185094639

==========

B-TS13-*E*

==========

P	0.402781785	1.510551929	-1.965438724
O	-0.750605166	1.095498919	-2.826508284
O	1.681557178	0.532911897	-2.000818491
C	2.150321245	0.034013245	-3.280825853
H	1.927035928	-1.035904169	-3.299031019
H	1.595926404	0.511917710	-4.094598770
C	3.635392904	0.298278183	-3.396599293
H	3.835431337	1.373324513	-3.403519630
H	4.173169136	-0.155862495	-2.560157061
H	4.014555454	-0.132470027	-4.327394009
S	1.243995070	3.291535378	-2.723348379
C	-0.264928490	4.101109028	-3.392592430
H	0.117746390	4.919922352	-4.008754253
H	-0.754213154	3.380589008	-4.050170898
C	-1.208816290	4.608828068	-2.312862158
H	-1.601615310	3.781883478	-1.714070678
H	-0.702072918	5.306825161	-1.641459703
H	-2.055536509	5.125513077	-2.775069237
C	0.048190825	1.581343532	-0.280369252
C	-0.095417812	2.230515242	0.771101773
H	-0.117365278	3.165278673	1.308142662
S	-0.689428747	1.299463868	2.969689608
C	-0.745359480	2.977905750	3.697237968
H	-1.463323236	2.985955954	4.522788525
H	-1.149963975	3.671668530	2.945997238
C	0.614458978	3.472991467	4.177322865
H	1.017822266	2.812638283	4.949946880
H	1.333574057	3.492980719	3.352719307
H	0.542237103	4.483590126	4.592827797

==========

C13-*E*

==========

P	-1.634551497	0.459206158	-1.631569173
O	-2.648618708	-0.614256632	-1.922025349
O	-2.229092163	1.328237095	-0.381905901
C	-1.458021235	2.406053517	0.183008954
H	-0.443555718	2.393491881	-0.228383136
H	-1.382982186	2.209257931	1.256203910
C	-2.129816847	3.740265290	-0.080020201
H	-3.159800306	3.735801152	0.287475674
H	-2.134018426	3.967609573	-1.150080935
H	-1.582255276	4.534049043	0.436739138
S	-1.657622399	1.922614820	-3.226519265
C	-3.425145233	2.411899201	-3.242385825
H	-3.744804409	2.563465423	-2.208317193
H	-4.011542895	1.595490885	-3.667966924
C	-3.579458807	3.691158461	-4.057579857
H	-3.231100066	3.551321311	-5.085466487
H	-3.007937091	4.512094327	-3.613747972
H	-4.631690737	3.986354242	-4.093838342
C	-0.012100977	-0.015100428	-1.243339376
C	0.947341735	0.622374763	-1.926482647
H	0.838883346	1.389671073	-2.705747804
S	2.693954633	0.311261548	-1.657582726
C	3.456259715	1.583554231	-2.730663209
H	3.117462775	1.422084299	-3.757823929
H	3.107304831	2.567389107	-2.404865612
C	4.975957123	1.492011122	-2.641610708
H	5.336655582	0.512862494	-2.969534560
H	5.325394547	1.661327651	-1.619153245
H	5.432031607	2.250778757	-3.282943426

==========

D13-*E*

==========

P	1.855233370	1.619987680	-0.916330567
O	2.830993543	2.741791695	-0.774696554
O	2.223739719	0.795058754	-2.252670067
C	1.427167253	-0.319791413	-2.725886997
H	0.453758549	-0.324581796	-2.225375627
H	1.256169307	-0.129409732	-3.787846784
C	2.162050140	-1.626421733	-2.508162014
H	3.154854286	-1.591020387	-2.964161292
H	2.264813335	-1.845264891	-1.441320051
H	1.596794805	-2.440933627	-2.970145964
S	1.875567781	0.245305674	0.659837805
C	3.655272506	-0.229049415	0.634408168
H	3.932453247	-0.480476301	-0.392443213
H	4.240001074	0.633586578	0.957571025
C	3.838548186	-1.418051851	1.569998491
H	3.535540097	-1.167436911	2.590855014
H	3.252110578	-2.278864657	1.235488013
H	4.892426864	-1.706366512	1.588983999
C	0.147934383	2.128152110	-1.026619420
C	-0.883015827	1.396829805	-0.572150397
H	-0.740158684	0.428742719	-0.086662199
S	-2.551211400	1.898077367	-0.704437478
C	-3.435814305	0.488026357	0.059272802
H	-3.107367808	0.394565360	1.096875716
H	-3.170486407	-0.421405059	-0.484893146
C	-4.932682686	0.766531325	-0.025954203
H	-5.198324419	1.684450140	0.506459374

H	-5.260729575	0.861365645	-1.065073554
H	-5.483427813	-0.060006901	0.429186722
H	0.001520533	3.092077421	-1.519617511

==========

14

==========

P	-1.209060226	-0.537085816	0.419622618
O	-2.602158183	-0.385664558	-0.062351594
O	-1.118822187	-1.658959595	1.547301720
C	0.149191951	-2.013138610	2.159902214
H	0.879042854	-1.215015973	1.984582529
H	0.504893621	-2.923368668	1.669773793
C	-0.079523096	-2.222806685	3.641356675
H	-0.835520912	-2.993794562	3.810521005
H	-0.408811615	-1.296187629	4.120830288
H	0.854977485	-2.542666664	4.109674418
O	-0.518606166	0.755768821	1.044655431
C	-1.125785661	1.390655136	2.206674486
H	-1.714425670	0.652073778	2.762398237
H	-1.800368023	2.170857424	1.845638053
C	-0.011096825	1.953610158	3.061207732
H	0.589937644	2.666723892	2.491020553
H	0.642094532	1.154844823	3.424907196
H	-0.439482270	2.471103444	3.923565886
C	-0.038478348	-0.977676141	-0.818429789
C	0.736174995	-1.322551163	-1.681450084
H	1.424296022	-1.628112028	-2.451384071

==========

B-TS14

==========

P	-1.070437759	0.744526421	-0.094709381
O	-2.471519837	1.188841229	-0.347207601
O	-1.039102722	-0.097833101	1.284500110
C	0.241793742	-0.494397954	1.825210725
H	0.737898830	0.389061597	2.241471765
H	0.860594486	-0.896978557	1.017420856
C	-0.001543951	-1.539216982	2.890531555
H	-0.483620263	-2.419743455	2.457830644
H	-0.635265970	-1.138722354	3.686467526
H	0.954257940	-1.845628668	3.324150286
O	0.000260037	1.922633987	0.151835607
C	-0.197439525	2.833330927	1.257037584
H	-0.642731635	2.293360183	2.100138667
H	-0.893663841	3.615538216	0.941573868
C	1.155317950	3.404398882	1.626854863
H	1.600433971	3.922181410	0.773326965
H	1.835621583	2.608880887	1.943690518
H	1.047757028	4.117263337	2.447863527
C	-0.306056805	-0.137739259	-1.360719337
C	0.136118131	-1.244646403	-1.734607780
H	0.570089823	-1.801307383	-2.552157339
S	0.275734994	-3.225736259	-0.383821471
C	0.801744586	-4.347311096	-1.730828165
H	1.013390044	-3.746982762	-2.628006503
H	1.750800451	-4.817961189	-1.456820259
C	-0.224705204	-5.421006041	-2.078355943
H	-1.168025256	-4.967957643	-2.396025328
H	-0.432959111	-6.058139908	-1.213916439
H	0.140245477	-6.059557968	-2.890427947

==========

C14

==========

P	-2.927216632	1.279613745	-2.883022619
O	-4.391955485	1.612119234	-2.994520338
O	-2.776605284	0.288798101	-1.579527209
C	-1.448511715	-0.054626475	-1.144755087
H	-0.947048101	0.846707806	-0.771269287
H	-0.874493230	-0.436766416	-1.996014648
C	-1.552947754	-1.103770487	-0.058071462
H	-2.031579456	-2.007641712	-0.444894186
H	-2.133064214	-0.729195750	0.790824981
H	-0.551458779	-1.364359364	0.297472912
O	-2.040268042	2.561726159	-2.394204890
C	-2.377815631	3.188039529	-1.145947134
H	-2.634508714	2.422495040	-0.405038084
H	-3.257089187	3.824567654	-1.290547900
C	-1.179999781	3.997190454	-0.692638292
H	-0.923648409	4.755844455	-1.436692246
H	-0.311780033	3.347935913	-0.547094517
H	-1.399690207	4.499108916	0.252766815
C	-2.079469778	0.781958643	-4.312977627
C	-1.924062577	-0.512062966	-4.602790779
H	-1.423617908	-0.857325662	-5.516915013
S	-2.511394150	-1.999883724	-3.713396847
C	-1.574820895	-3.311658451	-4.566908611
H	-2.098393381	-4.246973586	-4.347949270
H	-1.650994215	-3.144532389	-5.645695952
C	-0.119562959	-3.384617576	-4.123514229
H	-0.052330140	-3.568780785	-3.047815928
H	0.400017879	-2.446809125	-4.339542693
H	0.400621711	-4.193141966	-4.646021544

==========

D14

==========

P	0.986568877	-0.203573933	-0.200490904
O	2.420223133	-0.036147932	0.163808763
O	0.635490789	0.789817532	-1.417757891
C	-0.696241831	0.792514851	-1.984836601
H	-0.992523293	-0.238407723	-2.208233099
H	-1.393029478	1.195888608	-1.241582671
C	-0.667739893	1.639658727	-3.237787498
H	-0.362633629	2.663071572	-3.004349006
H	0.026842642	1.221092448	-3.971603507
H	-1.666681055	1.666682994	-3.681406672
O	0.554207182	-1.654586535	-0.722904621
C	1.146544072	-2.174771029	-1.942605855
H	1.324213310	-1.347317250	-2.638559215
H	2.109085478	-2.625584078	-1.685598245
C	0.190310372	-3.189127399	-2.531207705
H	-0.001261929	-3.996374139	-1.819765237
H	-0.762426918	-2.721172600	-2.794892391
H	0.626795762	-3.620021893	-3.436159058
C	-0.154500586	0.102099149	1.132038947
C	-1.396806751	-0.381568279	1.311520225
H	-1.955545338	-0.047100580	2.187143639
S	-2.272835448	-1.538019118	0.329456748
C	-3.921831096	-1.462325270	1.126565446
H	-4.278402682	-0.430212557	1.094738439
H	-3.820220353	-1.771236290	2.169936645
C	-4.865267016	-2.390195609	0.368084045
H	-4.973898400	-2.080705158	-0.675579055
H	-4.509219606	-3.424579526	0.386171094
H	-5.854312382	-2.365302787	0.832518935
H	0.224513524	0.803782807	1.873122912

==========

15

==========

P	4.037204994	-0.206530772	5.098352359

O	3.675410424	0.042608002	3.674748343
O	3.176075652	-1.307268074	5.881528347
C	3.216994296	-2.695154007	5.454990559
H	2.420555607	-2.844842492	4.720844918
H	4.178990723	-2.898342615	4.973995821
C	3.020165348	-3.564869265	6.678472902
H	3.825976273	-3.409991092	7.402306562
H	2.066445037	-3.339749402	7.163365107
H	3.017567460	-4.617433689	6.382006634
N	5.602859654	-0.673570926	5.291803161
C	6.161472645	-0.966922448	6.621058853
H	6.787515158	-0.133450336	6.957096545
H	5.328448328	-1.041473843	7.328122237
C	6.953000922	-2.268815358	6.626482249
H	6.312308414	-3.113466268	6.355211705
H	7.783432740	-2.225786985	5.915765350
H	7.365524118	-2.454451639	7.622697555
C	3.700697117	1.173915506	6.160954014
C	3.500788407	2.130007799	6.875984519
H	3.332977620	2.980457239	7.514347170
H	6.261291831	-0.331392496	4.592608278

==========

B-TS15

==========

P	3.898996199	-0.297745289	5.037135042
O	4.328359153	0.265902072	3.713244249
O	3.119466716	-1.718425725	4.960247547
C	3.789668857	-2.923608095	4.546744594
H	3.620069519	-3.061239955	3.474517959
H	4.864902567	-2.823497405	4.720125912
C	3.216367689	-4.077930567	5.345057061
H	3.417082024	-3.944720112	6.412135841
H	2.134796072	-4.147867145	5.201316384
H	3.668306324	-5.019390918	5.022566957
N	5.232624176	-0.679940528	5.974875927
C	5.027788157	-1.232693763	7.324704235
H	5.018406995	-0.423467862	8.062832900
H	4.035402400	-1.696977672	7.354665864
C	6.085130734	-2.274779598	7.669710315
H	6.051499860	-3.117204138	6.970778062
H	7.090294351	-1.842002553	7.635904235
H	5.917722032	-2.660814351	8.680314457
C	2.686378693	0.624241844	5.872766834
C	2.583391411	1.449183482	6.817430704
H	1.857607468	2.017900380	7.380387753
S	4.318841379	2.376299185	8.077466470
C	3.388905048	2.226707570	9.649409164
H	2.332403487	2.461968032	9.459464304
H	3.746484991	2.986634500	10.351014367
C	3.491283807	0.841484456	10.277667630
H	3.118881719	0.082043630	9.584051984
H	4.529433687	0.592710215	10.516617100
H	2.906316341	0.785142016	11.201871777
H	5.968179144	0.025197810	5.926051524

==========

C15

==========

P	3.537097467	-0.402274046	5.297339456
O	4.055586232	0.465996895	4.171712238
O	2.974589023	-1.841357010	4.753549016
C	3.867189869	-2.689030601	4.012663115
H	3.370220566	-2.932645992	3.068916654
H	4.791405749	-2.152845523	3.777150200
C	4.167723605	-3.947259299	4.805024138
H	4.743054948	-3.702365082	5.701592204
H	3.240475332	-4.442298477	5.107056190
H	4.749658421	-4.646831343	4.199172118
N	4.871833141	-0.936246699	6.219442334
C	4.567937953	-1.598467077	7.498340810
H	4.103232588	-0.901771316	8.208776658
H	3.832732386	-2.386875350	7.300570536
C	5.823012207	-2.196375542	8.118283782
H	6.287799756	-2.927052432	7.448660516
H	6.559565206	-1.413469966	8.331771981
H	5.580990794	-2.694681954	9.061972794
C	2.152836354	0.159409127	6.214788803
C	2.368033023	1.054625534	7.181587105
H	1.568735307	1.470399392	7.808512101
S	3.925548119	1.906138817	7.668346786
C	3.559586730	2.349290065	9.401828623
H	2.584927204	2.846847485	9.424339761
H	4.308083249	3.093727350	9.687801649
C	3.584680884	1.156411574	10.347580400
H	2.840527274	0.411308052	10.051004894
H	4.567365775	0.676341401	10.345225475
H	3.360049351	1.475948060	11.369926436
H	5.529599610	-0.168232731	6.359074881

==========

D15

==========

P	0.886284173	-0.168063670	-0.639487505
O	2.328506470	-0.383522868	-0.313244492
O	0.715574980	1.071070910	-1.656828761
C	1.467096686	1.163607478	-2.887020111
H	2.533336401	1.267843723	-2.653555393
H	1.328492999	0.242236391	-3.461905718
C	0.961209655	2.367703915	-3.650249720
H	-0.098739319	2.249878407	-3.890128851
H	1.093035817	3.279695749	-3.062330484
H	1.521781921	2.469036818	-4.583262920
N	0.198122248	-1.433871388	-1.466930628
C	-1.190700769	-1.322925329	-1.936903358
H	-1.516720176	-0.291485697	-1.767858148
H	-1.258709908	-1.516429663	-3.015047789
C	-2.087664843	-2.286803484	-1.174445391
H	-1.762699246	-3.321208477	-1.329825282
H	-2.060335636	-2.073698044	-0.102437310
H	-3.119611502	-2.199365139	-1.524109364
H	0.795330405	-2.047982454	-2.019596815
C	-0.030717185	0.219757184	0.854816258
C	-0.886295259	1.230809093	1.084932685
H	-1.356373310	1.306211352	2.066874981
S	-1.367242575	2.505306721	-0.018410286
C	-2.474392414	3.491436005	1.058308721
H	-1.900290012	3.831679821	1.923335791
H	-3.288095713	2.847617626	1.400466800
C	-3.006373405	4.670816898	0.251525193
H	-2.192723036	5.314767838	-0.094785169
H	-3.575282574	4.333569527	-0.619837940
H	-3.670561790	5.271594524	0.878111064
H	0.147526681	-0.474464387	1.674640894

Table S6. Vibrational frequencies (in cm^{-1}) of the optimized structures

==========
EtSH
==========
203.30 264.23 304.67 686.92 792.32 873.82
1012.49 1059.26 1123.54 1277.18 1314.20 1428.45
1505.28 1510.67 1519.48 2727.06 3082.96 3114.69
3156.42 3164.70 3179.27
==========
EtS^-
==========
219.74 320.97 666.20 745.39 984.41 993.16
1065.93 1257.62 1264.54 1386.38 1490.51 1492.70
1511.96 3047.67 3059.06 3083.42 3127.98 3154.78
==========
10
==========
42.80 44.31 74.72 89.48 98.06 122.41
159.12 209.02 232.48 251.46 269.47 286.76
298.82 344.53 391.35 425.17 500.94 561.36
638.83 687.14 763.88 793.40 797.32 816.35
981.38 1005.91 1021.46 1032.91 1041.88 1066.84
1086.41 1093.71 1128.10 1193.43 1255.94 1274.28
1287.43 1310.85 1322.67 1402.74 1426.20 1439.83
1440.32 1499.03 1500.64 1509.61 1512.20 1516.39
1531.74 1708.86 3080.46 3081.43 3100.57 3107.14
3152.01 3159.90 3163.61 3165.70 3170.11 3174.44
3183.25 3198.32 3263.85
==========
B-TS10
==========
-122.44 11.47 27.93 41.54 42.78 47.00
60.29 82.82 86.51 103.22 121.98 153.72
224.86 245.53 250.70 252.04 260.12 287.35
290.11 322.90 335.73 371.64 421.71 475.15
476.29 536.71 644.80 693.52 694.59 764.14
769.13 780.94 809.76 827.99 923.14 982.28
1002.40 1002.71 1027.57 1050.86 1063.15 1074.72
1081.01 1102.97 1121.30 1140.01 1183.86 1209.09
1247.94 1260.87 1271.19 1289.51 1295.61 1304.71
1363.09 1393.79 1407.24 1414.02 1430.36 1496.84
1497.24 1498.64 1503.13 1506.41 1511.76 1516.72
1517.86 1519.24 1535.76 3056.48 3063.04 3065.76
3074.63 3079.00 3098.20 3103.56 3114.34 3133.59
3148.53 3153.81 3154.25 3155.40 3161.16 3167.85
3173.94 3192.68 3246.98
==========
C10
==========
18.11 26.59 41.22 47.68 58.77 72.47
82.08 99.41 121.77 128.26 160.96 189.18
223.31 239.19 247.76 257.44 276.29 282.02
297.95 344.05 355.52 404.08 466.57 475.38
504.61 595.91 647.83 693.99 707.87 757.69
776.03 783.14 824.32 830.29 945.24 980.43
999.57 1004.60 1037.27 1043.89 1076.88 1077.45
1100.89 1122.60 1140.79 1158.86 1185.07 1197.53
1247.34 1258.32 1263.68 1288.61 1300.58 1301.98
1350.50 1390.86 1410.73 1414.15 1426.89 1472.74
1494.97 1498.38 1500.22 1505.68 1507.73 1516.88
1518.84 1519.22 1539.57 3059.04 3068.16 3069.82
3073.69 3075.42 3077.72 3106.34 3107.31 3119.18
3143.38 3144.94 3147.77 3147.90 3158.87 3160.71
3166.22 3171.00 3175.85
==========
D10
==========
30.56 37.19 44.22 48.39 63.43 66.45
82.93 107.88 112.60 134.72 152.72 200.91
226.39 254.73 255.48 265.26 267.57 294.25
312.50 335.67 343.75 411.67 453.63 483.29
543.45 685.47 702.85 710.40 730.96 783.47
794.55 811.10 822.19 868.48 941.91 990.81
1003.38 1008.87 1045.38 1057.86 1066.94 1085.18
1088.87 1099.76 1133.24 1147.94 1185.18 1203.33
1242.11 1266.95 1271.13 1296.28 1307.82 1315.64
1334.23 1343.91 1403.51 1425.45 1427.75 1439.17
1461.47 1490.05 1490.06 1499.88 1502.12 1508.68
1510.88 1515.77 1516.59 1519.44 1528.50 3077.49
3080.10 3080.23 3081.07 3083.02 3087.30 3091.92
3124.45 3135.46 3135.62 3138.31 3155.50 3158.62
3161.16 3163.16 3166.41 3168.06 3172.45 3192.09
==========
13
==========
48.90 74.29 84.89 106.36 127.20 140.36
155.04 214.46 259.97 282.63 287.10 298.88
319.10 385.20 432.75 447.25 458.49 582.87
687.46 716.63 785.42 787.39 793.57 794.38
819.88 976.22 1005.81 1068.19 1073.36 1090.68
1124.59 1195.48 1266.20 1274.69 1309.47 1321.05
1398.38 1426.67 1434.97 1494.25 1501.14 1509.04
1514.94 1516.64 1534.53 2211.94 3079.49 3080.63
3103.22 3108.88 3153.99 3156.58 3165.10 3165.73
3175.25 3177.92 3412.14
==========
B-TS13
==========
-133.81 13.41 20.60 30.61 39.76 51.03
59.49 74.47 87.36 154.60 159.14 166.15
205.98 223.58 242.18 263.18 266.62 299.67
329.55 333.16 357.43 388.66 422.55 446.80
487.18 557.29 681.26 681.55 740.36 748.50
753.72 767.70 794.59 813.32 945.19 978.15
992.20 998.41 1025.37 1063.18 1078.18 1094.04
1098.71 1130.48 1190.23 1241.78 1272.99 1281.36
1285.51 1308.31 1317.75 1396.89 1405.38 1427.75
1435.83 1483.55 1489.40 1496.54 1498.58 1499.47
1505.26 1511.23 1514.40 1525.82 2000.71 3021.02
3058.00 3073.56 3080.96 3095.87 3098.96 3107.61
3132.20 3142.73 3152.78 3156.23 3161.38 3163.29
3172.36 3180.47 3317.85
==========
C13
==========
12.89 30.56 40.19 62.65 73.67 77.99
92.29 97.17 110.43 135.75 165.64 202.88
225.62 245.19 251.14 263.27 279.28 326.94
337.45 366.75 419.14 426.17 458.09 531.02
540.61 661.67 692.63 718.70 727.50 781.29
782.50 790.07 801.30 828.90 949.59 1000.68
1006.64 1039.47 1049.27 1080.30 1082.96 1094.91
1127.97 1193.92 1206.71 1259.75 1263.64 1280.50
1290.37 1317.23 1324.47 1392.83 1411.60 1417.26
1431.75 1494.05 1498.24 1500.30 1505.69 1508.55
1513.50 1515.83 1519.39 1530.63 1647.92 3071.15
3072.92 3073.46 3074.19 3082.74 3086.14 3104.68
3128.34 3135.35 3146.36 3147.82 3148.54 3152.33
3160.72 3164.40 3172.94
==========
D13
==========
33.52 45.59 56.61 68.99 71.21 78.22
87.42 104.00 121.11 153.17 157.35 205.29
222.53 262.53 264.90 272.10 291.12 300.65
333.85 377.94 398.43 414.16 472.65 548.87
585.00 678.20 692.69 704.08 712.31 791.53
798.83 808.87 826.73 872.24 988.53 989.48
1004.71 1008.21 1057.75 1066.46 1090.92 1092.73

1105.49 1138.33 1183.99 1209.20 1246.94 1271.49
1272.40 1300.81 1307.55 1319.43 1365.08 1405.29
1425.20 1430.03 1440.54 1500.12 1500.60 1500.97
1509.38 1510.85 1514.17 1516.45 1518.22 1528.16
1652.88 3075.73 3081.09 3081.34 3083.08 3103.41
3114.10 3129.60 3153.92 3160.58 3163.25 3164.39
3164.69 3167.54 3173.39 3173.83 3184.39 3191.41

B-TS13-*E*

-154.76 19.83 27.46 36.39 42.17 45.54
65.88 73.26 90.94 103.26 158.68 177.56
191.44 207.19 243.99 260.49 262.83 293.84
331.36 332.58 370.29 385.02 403.69 449.66
488.15 558.04 677.75 683.29 745.31 754.71
759.06 767.69 798.77 819.14 960.78 978.76
991.22 1001.63 1024.15 1064.17 1078.87 1086.40
1094.69 1130.47 1191.13 1235.99 1270.83 1280.38
1285.97 1311.39 1317.61 1395.79 1406.85 1423.54
1435.01 1482.51 1493.56 1499.25 1499.27 1503.08
1512.96 1513.58 1513.84 1529.50 1982.92 3027.42
3061.83 3074.82 3079.64 3094.00 3102.64 3103.43
3135.91 3141.13 3151.56 3156.80 3160.29 3161.03
3172.25 3178.59 3304.24

C13-*E*

16.67 20.75 54.99 57.96 68.44 78.65
88.33 115.06 129.25 148.49 164.71 200.35
241.51 242.97 249.65 270.13 280.13 299.59
305.98 359.68 380.45 424.26 455.75 456.44
532.38 699.98 704.75 735.69 782.61 790.02
792.74 800.80 835.30 845.76 950.49 1000.66
1011.04 1044.96 1051.50 1082.37 1084.75 1098.81
1127.72 1195.87 1208.54 1262.16 1265.88 1291.92
1292.87 1323.77 1350.14 1390.88 1413.07 1415.60
1427.49 1495.08 1498.07 1503.13 1504.90 1508.38
1515.15 1517.64 1519.08 1531.11 1597.58 3031.29
3070.71 3074.43 3077.17 3086.97 3087.60 3109.27
3133.13 3136.47 3146.17 3149.06 3152.20 3153.16
3162.93 3166.94 3173.03

D13-*E*

26.53 36.53 55.77 62.95 79.21 89.80
95.62 122.52 124.21 167.73 185.75 194.36
244.94 250.79 261.41 274.72 286.34 290.01
306.06 362.88 387.76 419.78 445.21 465.68
557.14 684.46 706.63 763.43 792.38 799.30
803.12 808.31 862.94 863.83 967.13 1000.02
1001.70 1008.60 1059.72 1065.80 1090.05 1092.33
1094.71 1126.24 1194.34 1207.60 1255.64 1269.90
1272.25 1300.72 1306.60 1324.83 1328.34 1398.56
1425.31 1430.22 1434.54 1495.33 1501.32 1502.17
1508.28 1511.18 1515.09 1516.58 1518.33 1531.00
1655.43 3078.74 3081.29 3082.73 3099.70 3104.47
3115.68 3148.65 3154.86 3155.62 3163.36 3163.80
3165.52 3167.69 3169.19 3174.23 3175.16 3185.06

14

42.00 55.04 93.96 95.90 128.91 167.83
201.55 212.57 267.13 292.89 325.30 349.79
383.31 410.38 435.74 497.74 523.30 694.78
785.87 792.79 796.93 807.31 817.71 847.09
986.79 1004.72 1082.64 1107.13 1129.77 1131.58
1187.86 1193.78 1295.39 1319.54 1329.53 1406.01
1407.58 1441.33 1442.69 1498.30 1498.83 1509.29
1515.64 1528.18 1530.67 2217.93 3080.80 3082.27
3086.82 3088.88 3141.24 3146.58 3166.45 3167.26
3173.57 3174.68 3412.43

B-TS14

-111.14 26.06 39.06 46.63 63.12 70.31
90.65 110.49 145.35 147.92 153.16 177.77
223.20 247.66 257.40 263.72 296.82 320.11
328.92 352.00 394.52 429.38 460.16 514.20
533.44 686.76 736.89 740.96 753.35 808.84
813.60 821.40 843.04 971.36 985.86 993.95
999.15 1037.73 1077.83 1092.64 1108.80 1131.88
1142.21 1185.98 1188.30 1265.36 1279.12 1297.35
1303.64 1320.02 1393.35 1399.94 1405.95 1432.73
1441.76 1485.78 1494.02 1498.09 1500.77 1510.47
1515.03 1515.77 1524.97 1535.51 1974.65 3018.76
3060.23 3074.27 3079.45 3082.52 3083.39 3095.98
3132.18 3133.69 3136.19 3159.08 3160.64 3166.09
3170.07 3175.22 3291.86

C14

11.83 34.73 52.58 57.97 78.50 105.50
116.46 148.47 170.13 176.60 185.26 227.52
243.73 264.80 269.39 302.62 323.97 343.25
349.96 401.21 452.28 474.42 545.05 555.37
659.44 695.03 726.66 766.00 796.65 800.76
807.52 817.82 830.82 956.08 971.17 995.63
1047.56 1085.32 1097.59 1111.75 1132.53 1138.63
1182.20 1186.05 1211.44 1276.32 1292.20 1296.84
1310.86 1319.20 1388.79 1392.46 1410.01 1427.58
1433.06 1479.90 1495.95 1497.18 1502.27 1509.63
1513.86 1516.17 1524.91 1538.87 1612.09 3043.21
3064.01 3070.30 3072.32 3076.02 3079.91 3085.33
3118.32 3119.12 3132.80 3146.26 3149.47 3161.10
3164.65 3166.17 3166.55

D14

46.55 54.04 59.09 76.69 81.53 89.14
108.99 125.72 135.22 168.92 194.84 226.28
244.32 262.01 268.56 291.42 325.47 341.24
363.50 411.33 423.05 486.57 527.20 595.82
702.62 709.23 715.32 778.09 798.65 814.34
820.70 845.13 886.33 988.43 993.75 995.19
1009.69 1057.73 1087.55 1092.44 1108.01 1131.75
1139.68 1184.68 1186.98 1210.25 1272.74 1275.27
1304.00 1314.56 1319.41 1372.44 1403.55 1405.95
1429.29 1439.00 1442.72 1498.09 1501.04 1502.16
1509.36 1511.07 1515.11 1518.56 1528.56 1534.27
1657.32 3076.52 3080.38 3082.26 3082.82 3087.51
3101.89 3127.05 3141.54 3151.64 3163.48 3163.91
3165.49 3166.80 3171.09 3173.01 3173.97 3203.44

15

41.84 61.27 86.70 97.78 134.61 176.85
196.38 219.26 265.70 297.23 320.69 347.52
383.97 424.00 436.32 489.04 522.13 566.27
686.57 776.84 782.22 784.29 799.27 818.04
880.46 975.39 1000.18 1093.42 1111.84 1130.10
1133.34 1152.84 1187.75 1263.18 1315.94 1318.20
1391.72 1404.47 1429.26 1439.56 1459.38 1498.49
1502.66 1506.61 1514.74 1520.10 1530.53 2210.30
3074.19 3079.43 3081.18 3094.53 3127.30 3143.72
3157.79 3161.17 3163.78 3171.10 3414.27 3560.40

B-TS15

-130.33 22.58 32.19 51.80 63.32 70.02
80.91 97.71 120.48 152.29 158.47 193.23
223.70 254.59 269.56 278.52 300.21 313.83
339.11 369.09 415.83 419.28 461.09 494.65
531.53 607.56 684.03 726.08 736.06 752.00
790.00 797.28 812.41 867.05 958.96 976.04

992.38 1008.23 1042.19 1079.70 1102.91 1110.57
1130.35 1130.77 1147.21 1188.11 1229.15 1274.53
1289.22 1307.21 1308.50 1384.04 1393.00 1401.81
1417.16 1429.06 1443.74 1487.57 1496.07 1498.43
1503.85 1506.67 1513.72 1516.03 1524.61 1529.08
1917.08 3034.55 3061.43 3062.37 3079.35 3081.28
3087.14 3101.24 3121.61 3135.36 3136.45 3142.71
3148.04 3156.79 3161.21 3167.54 3282.46 3547.61

==========

C15

==========

32.97 39.69 50.85 74.84 81.55 105.05
115.86 149.72 165.48 174.64 198.81 233.04
256.45 263.80 275.50 286.38 333.55 342.62
376.46 401.53 448.26 483.46 522.29 553.37
636.60 689.56 692.54 722.30 762.36 783.32
800.15 802.04 817.47 859.11 948.88 952.29
996.74 1046.43 1084.57 1094.77 1100.14 1128.67
1138.12 1142.20 1180.38 1202.34 1274.62 1288.88
1296.01 1311.05 1317.62 1375.15 1386.38 1409.30
1411.72 1423.58 1437.10 1479.21 1494.44 1499.74
1502.51 1507.47 1513.39 1513.79 1521.86 1529.35
1594.31 3045.73 3060.84 3064.36 3068.28 3079.98
3084.32 3085.82 3108.78 3132.30 3132.42 3138.92
3143.43 3147.68 3157.79 3162.81 3174.10 3531.55

==========

D15

==========

39.70 60.74 65.58 71.37 83.77 87.26
111.02 118.25 144.82 165.24 198.95 222.17
244.05 260.32 264.84 298.54 323.86 341.58
356.59 370.64 456.62 474.37 489.61 521.66
594.91 689.69 708.30 712.78 760.91 794.06
797.45 816.14 866.95 882.11 965.96 983.83
992.32 1011.10 1056.89 1091.61 1104.53 1115.34
1127.21 1134.00 1161.83 1188.16 1211.70 1243.75
1273.87 1304.15 1314.54 1321.73 1373.06 1395.59
1402.26 1427.96 1428.54 1430.85 1438.95 1497.95
1500.32 1501.85 1504.72 1510.73 1512.99 1518.50
1519.40 1533.00 1665.61 3074.30 3076.52 3080.65
3081.10 3081.72 3100.39 3125.12 3132.16 3151.20
3155.49 3160.00 3162.47 3163.87 3168.05 3170.67
3171.49 3195.56 3587.34

7.2. NMR spectra

^{1}H-NMR spectrum of compound **1** in CD_3CN (300 MHz):

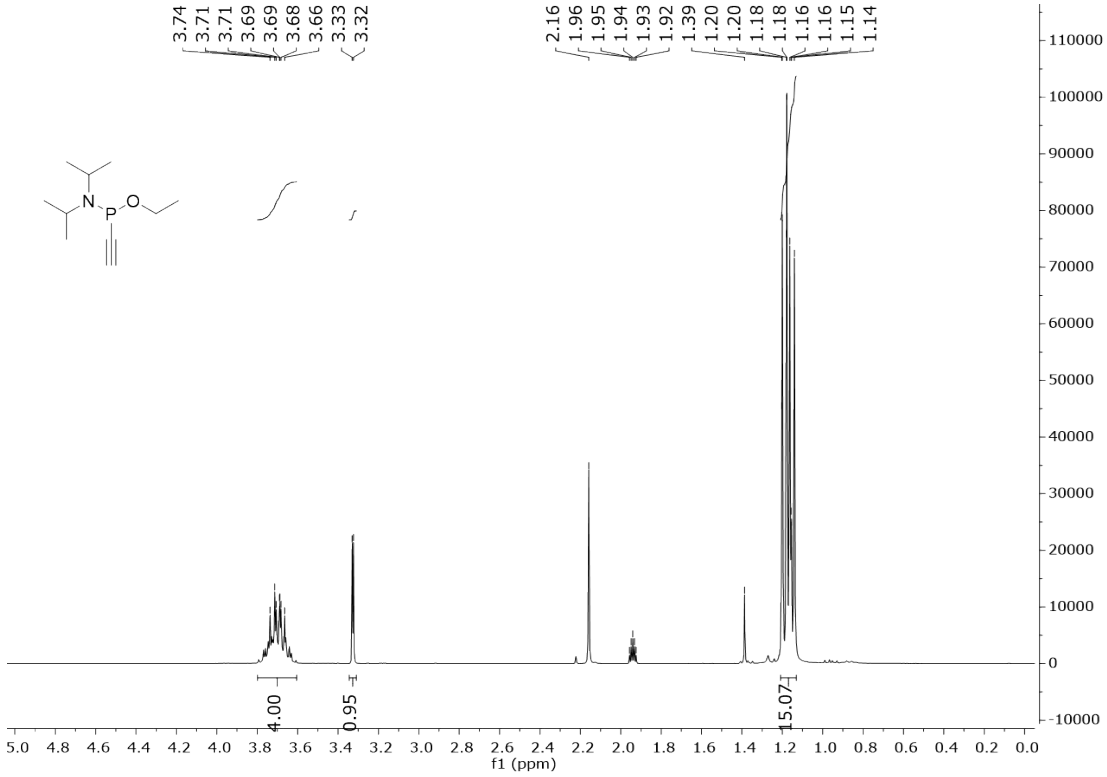

^{13}C-NMR spectrum of compound **1** in CD_3CN (75 MHz):

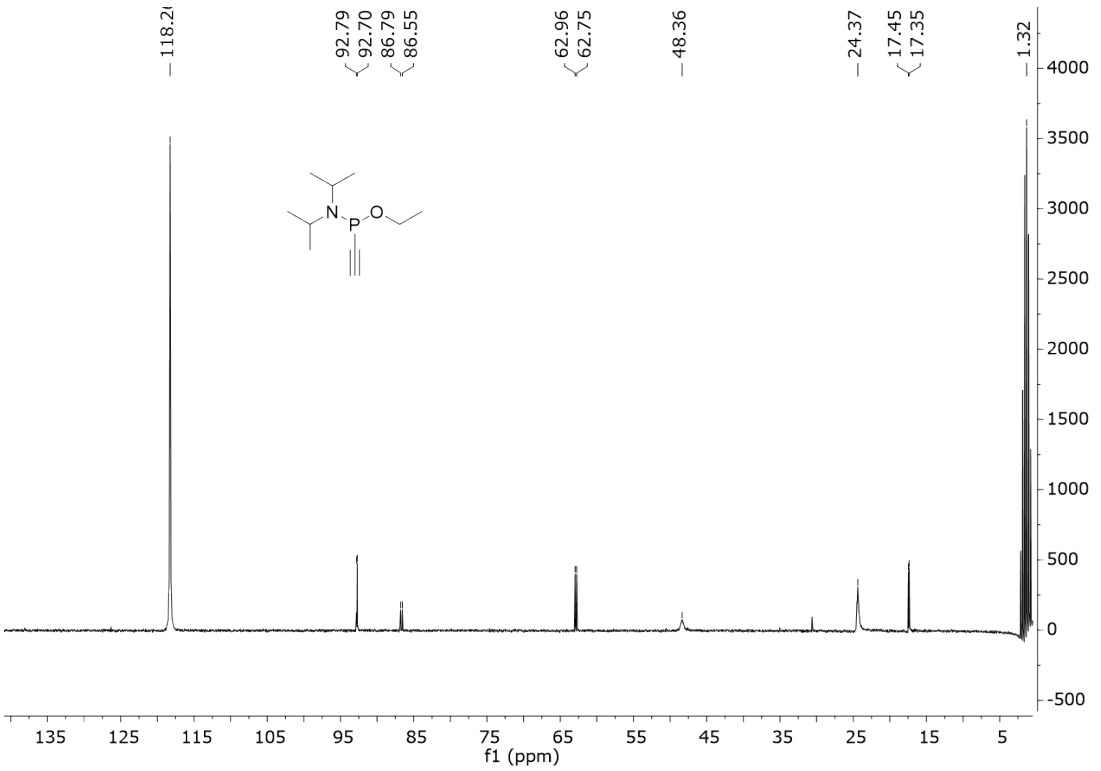

^{31}P-NMR spectrum of compound **1** in CD_3CN (122 MHz)

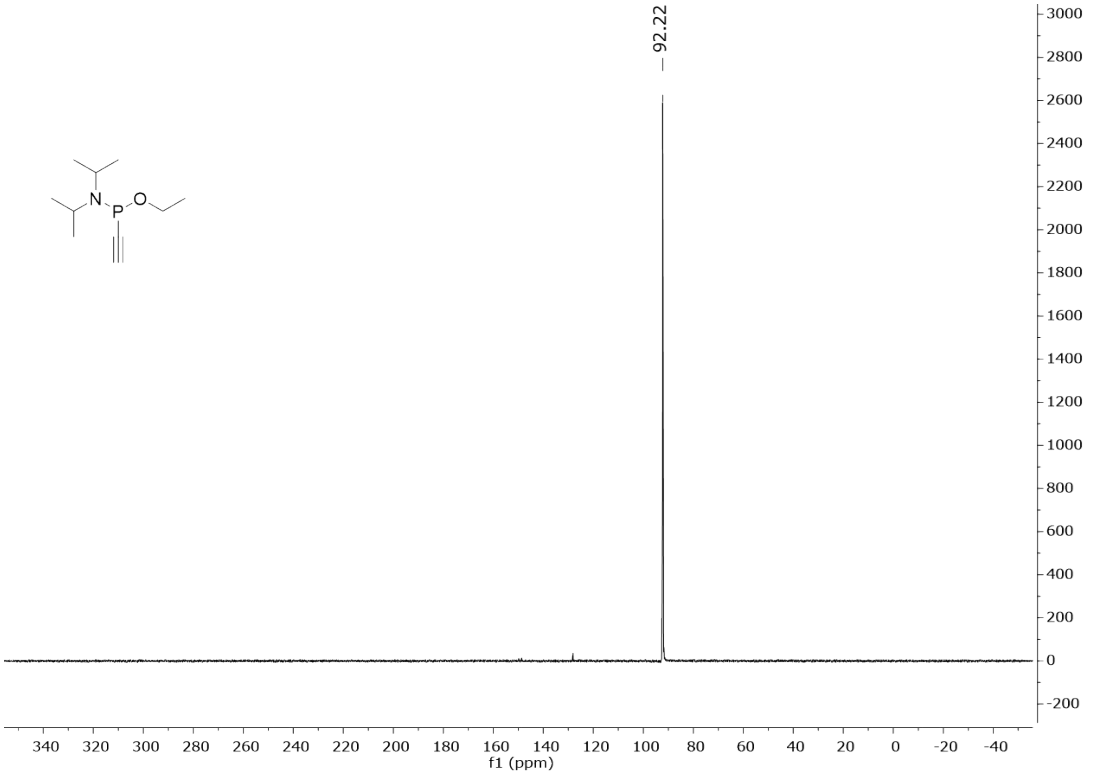

^{1}H-NMR spectrum of compound **4** in DMSO-d_6 (600 MHz):

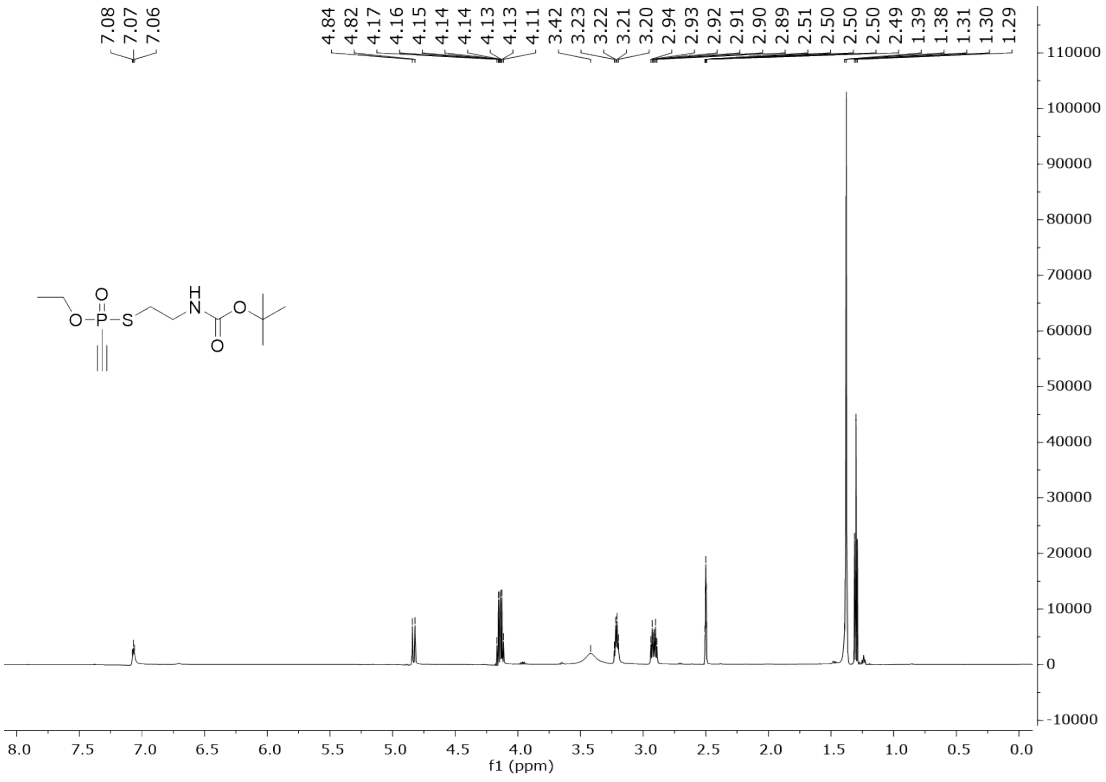

^{13}C-NMR spectrum of compound **4** in DMSO-d_6 (151 MHz):

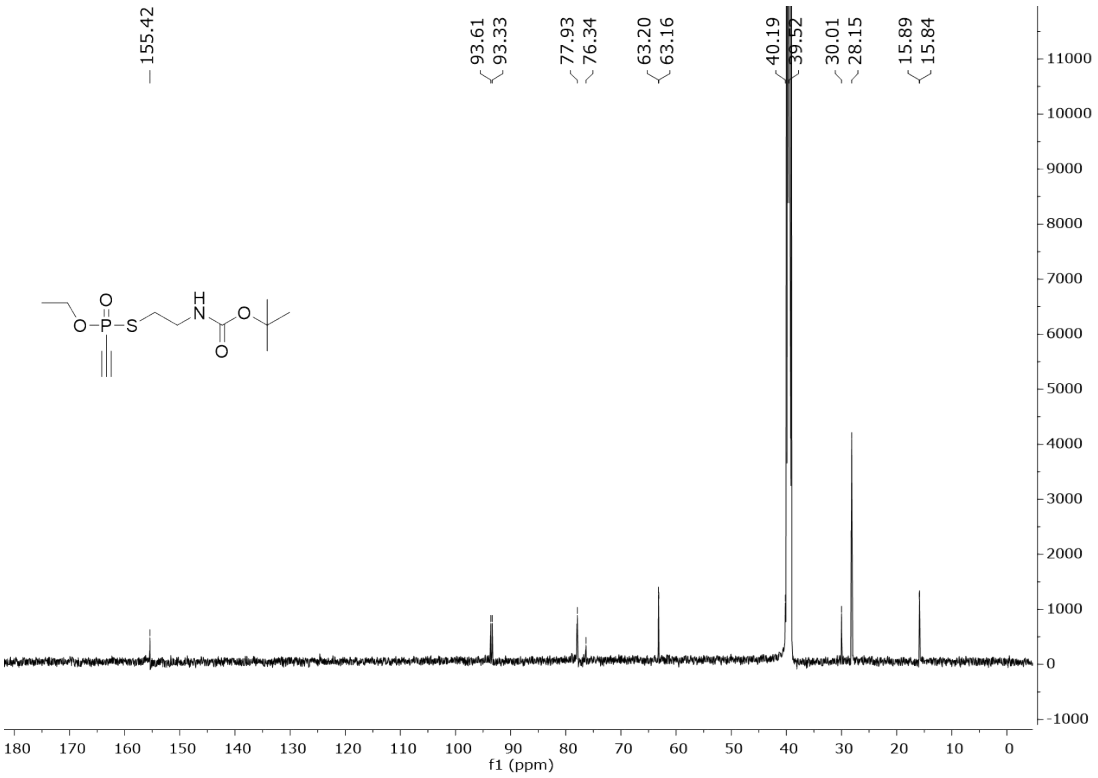

^{31}P-NMR spectrum of compound **4** in DMSO-d_6 (243 MHz):

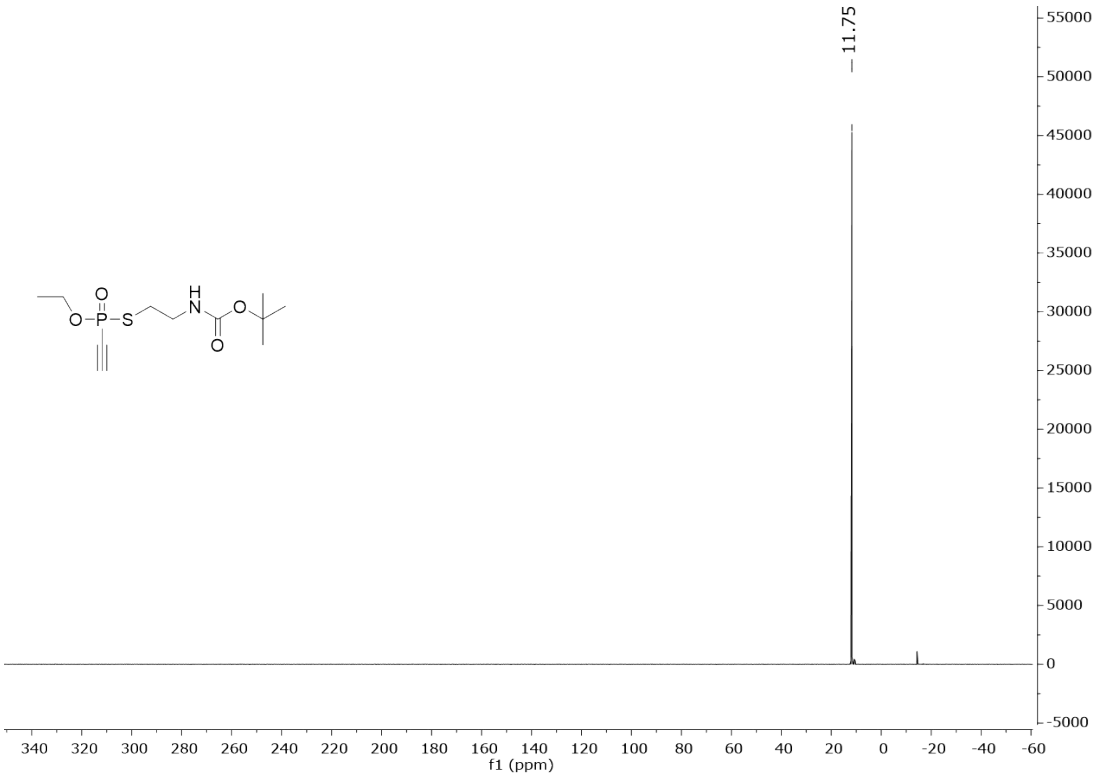

^{1}H-NMR spectrum of compound **5** in $CDCl_3$ (300 MHz):

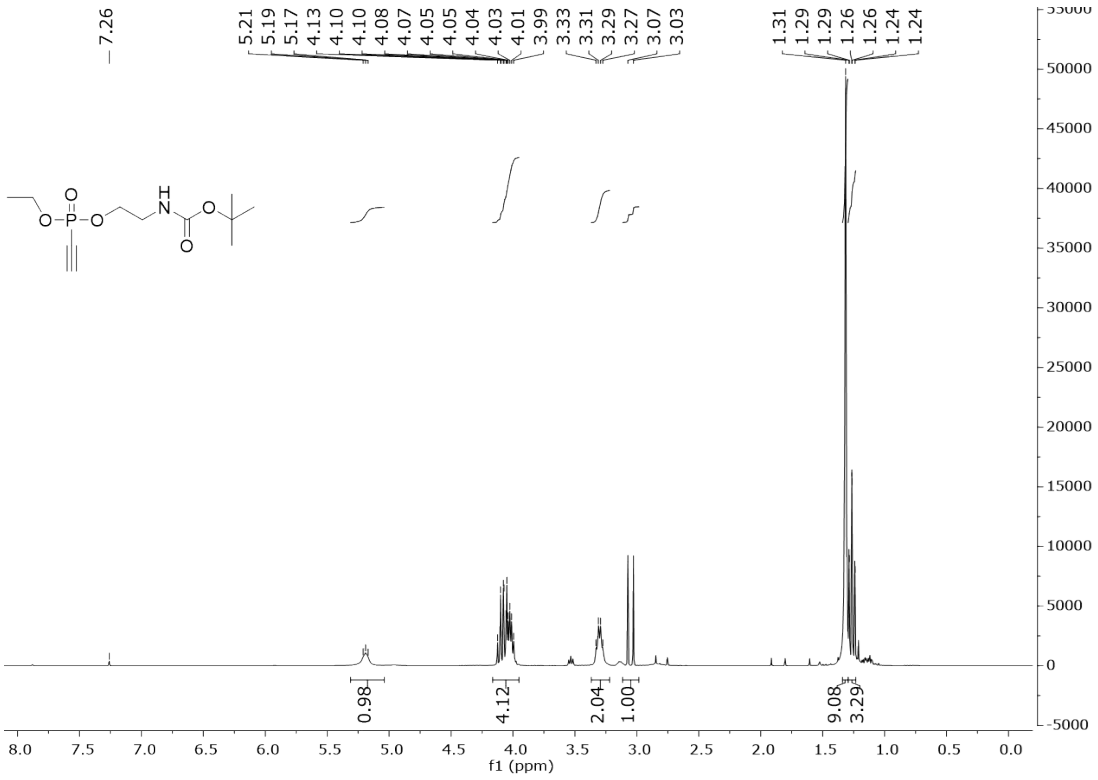

^{13}C-NMR spectrum of compound **5** in $CDCl_3$ (75 MHz):

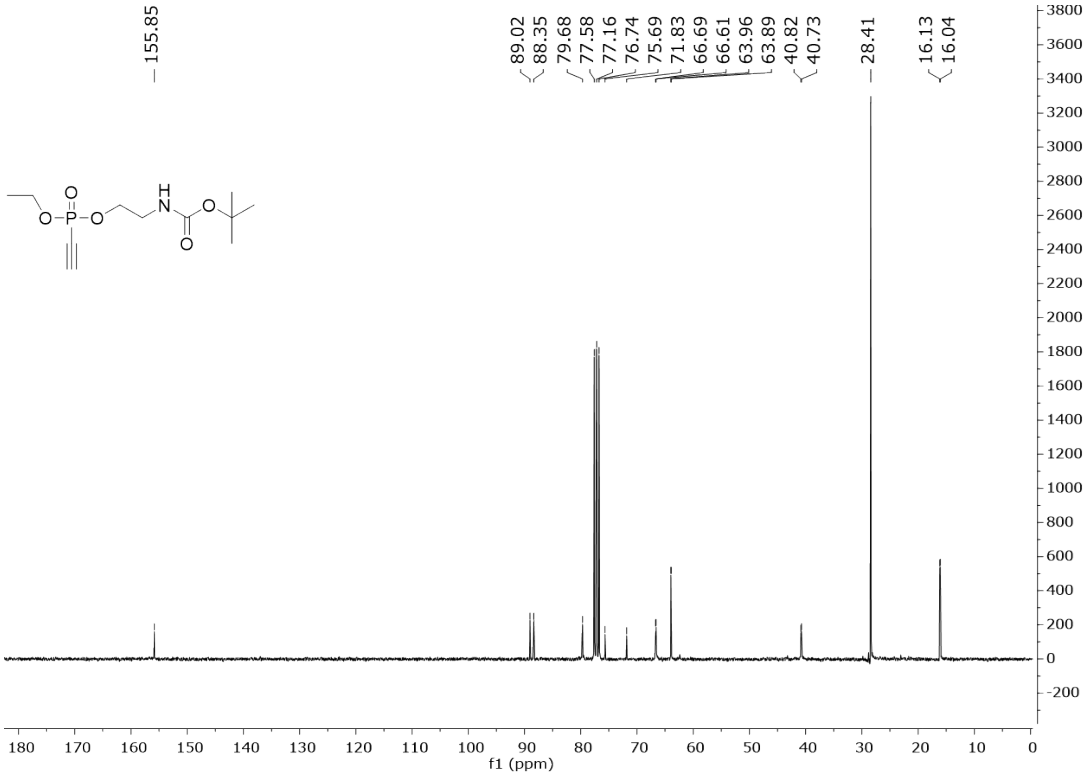

^{31}P-NMR spectrum of compound **5** in $CDCl_3$ (122 MHz):

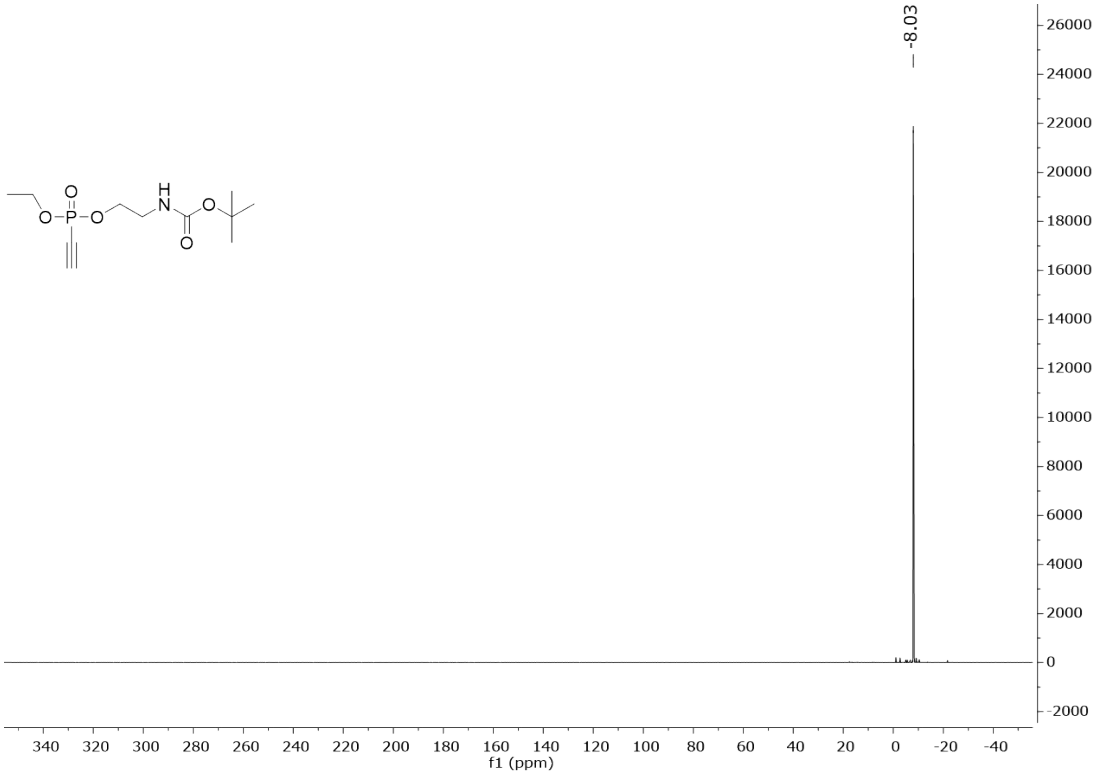

^{1}H-NMR spectrum of compound **7** in DMSO-d_6 (600 MHz):

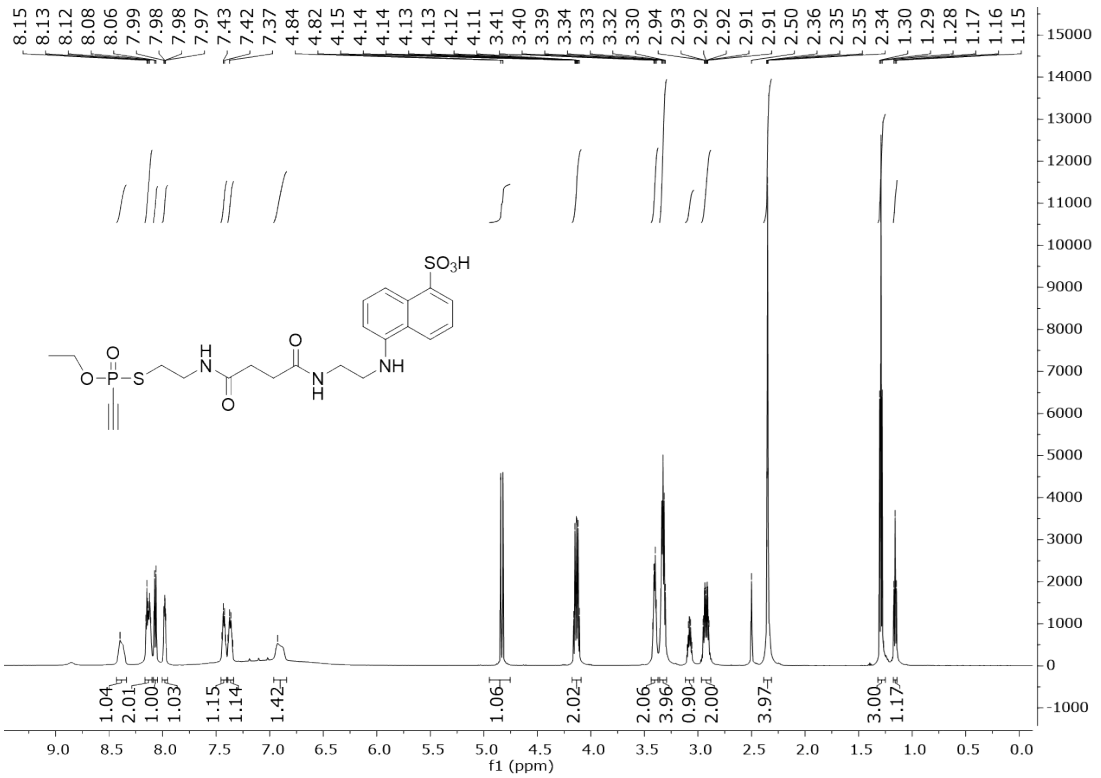

^{13}C-NMR spectrum of compound **7** in DMSO-d_6 (151 MHz):

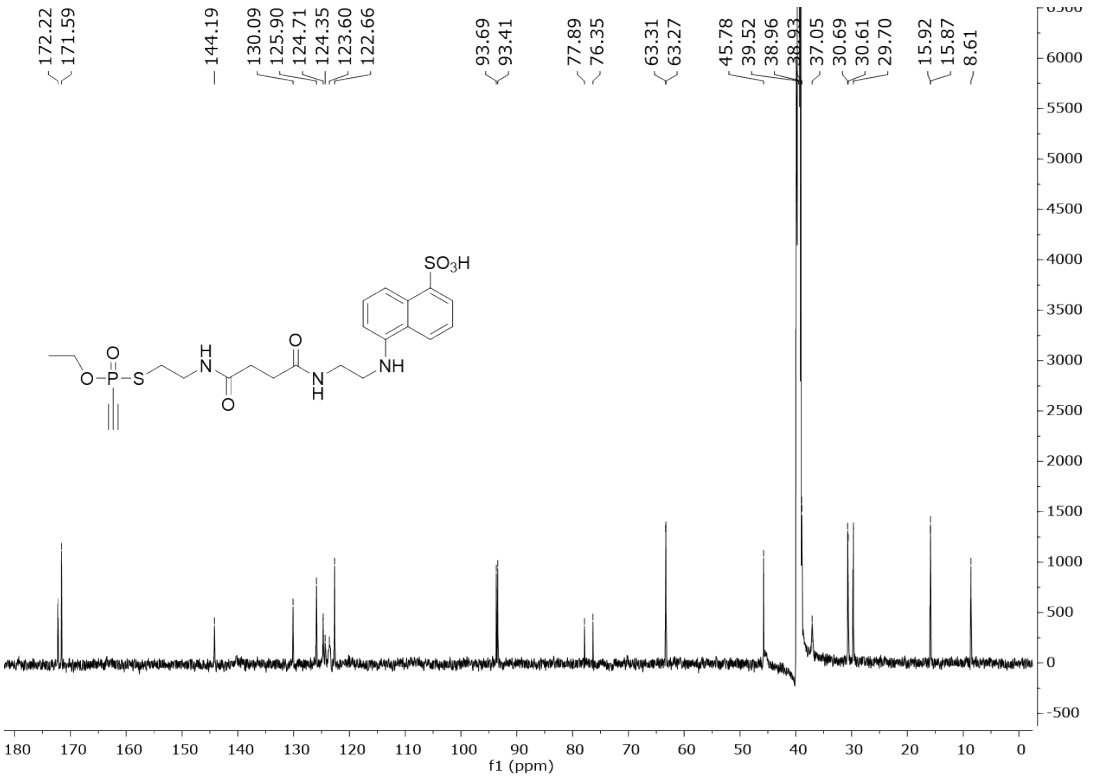

^{31}P-NMR spectrum of compound **7** in DMSO-d_6 (243 MHz):

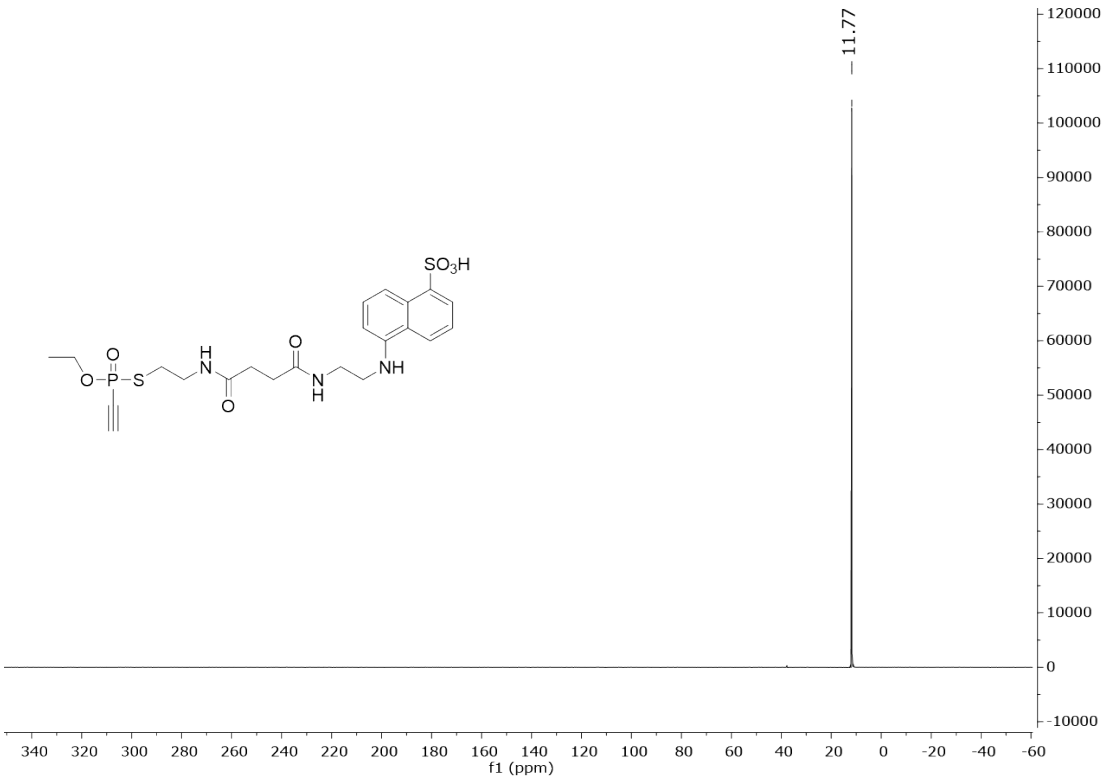

^{1}H-NMR spectrum of compound **8** in DMSO-d_6 (600 MHz):

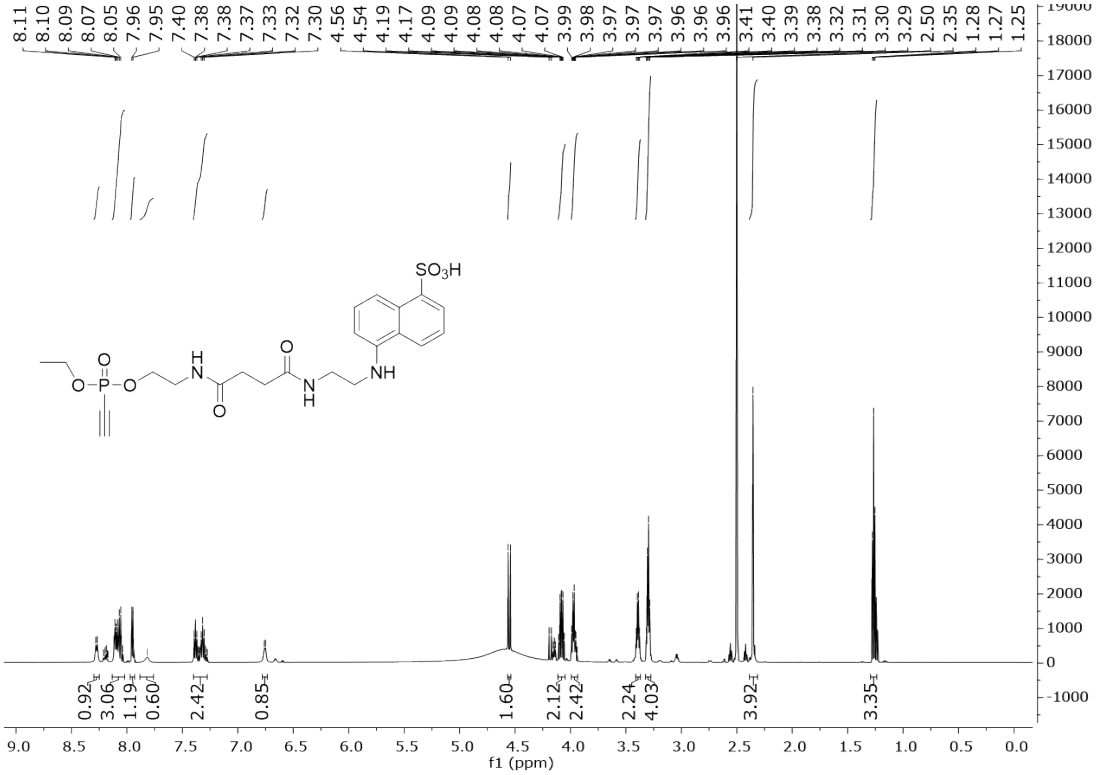

^{13}C-NMR spectrum of compound **8** in DMSO-d_6 (151 MHz):

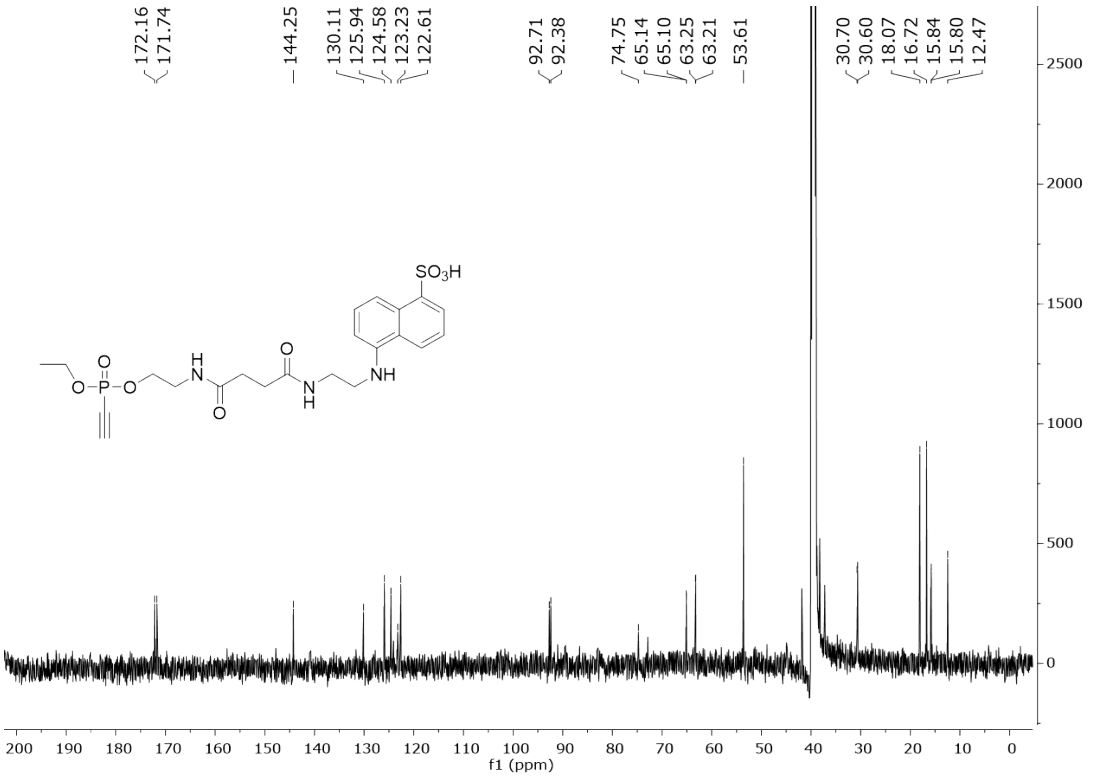

^{31}P-NMR spectrum of compound **8** in DMSO-d_6 (243 MHz):

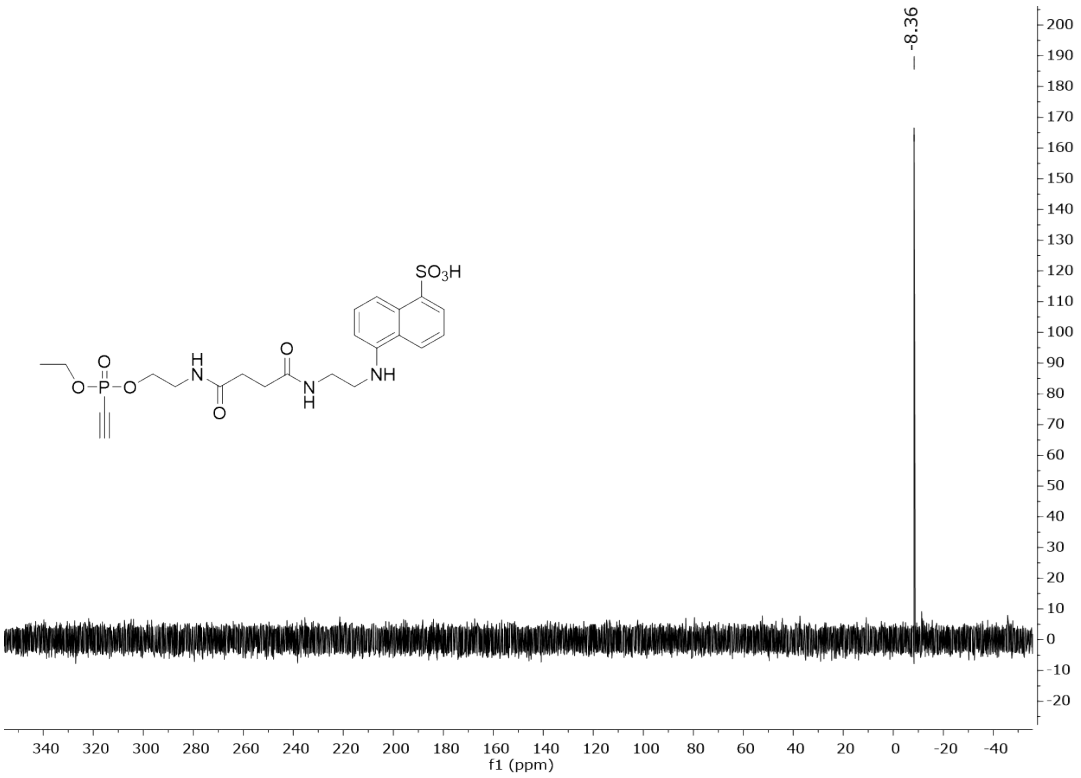

^{1}H-NMR spectrum of compound **13** in $CDCl_3$ (300 MHz):

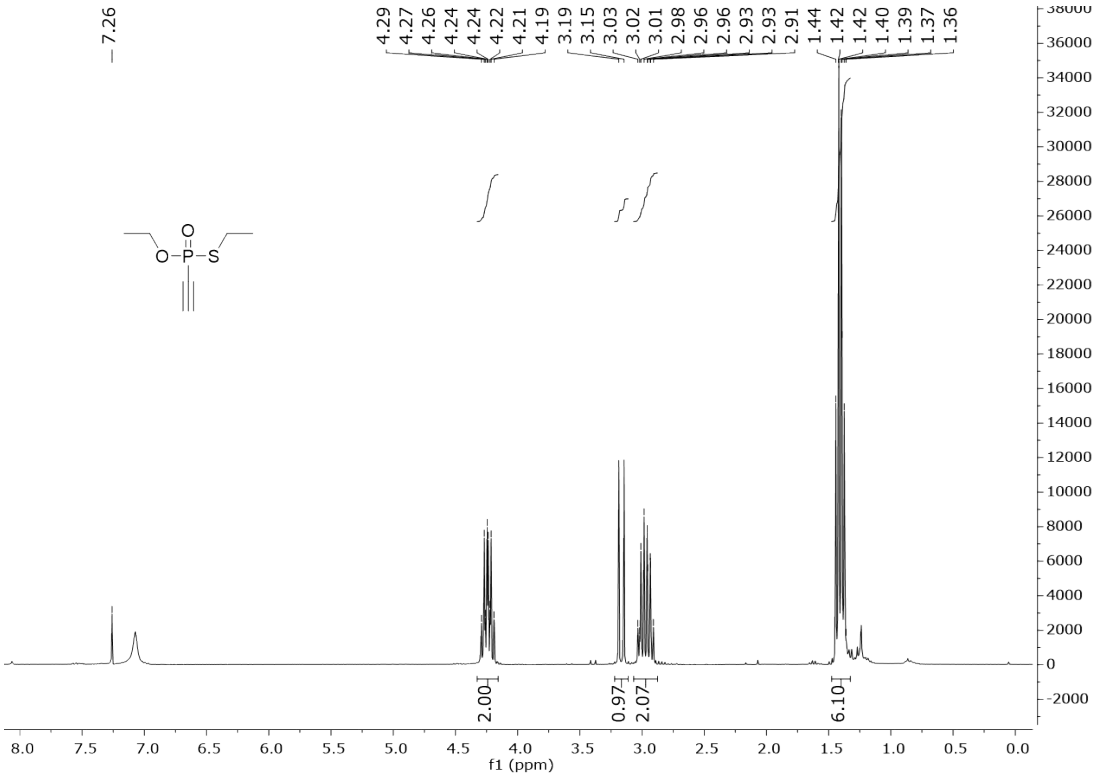

^{13}C-NMR spectrum of compound **13** in $CDCl_3$ (75 MHz):

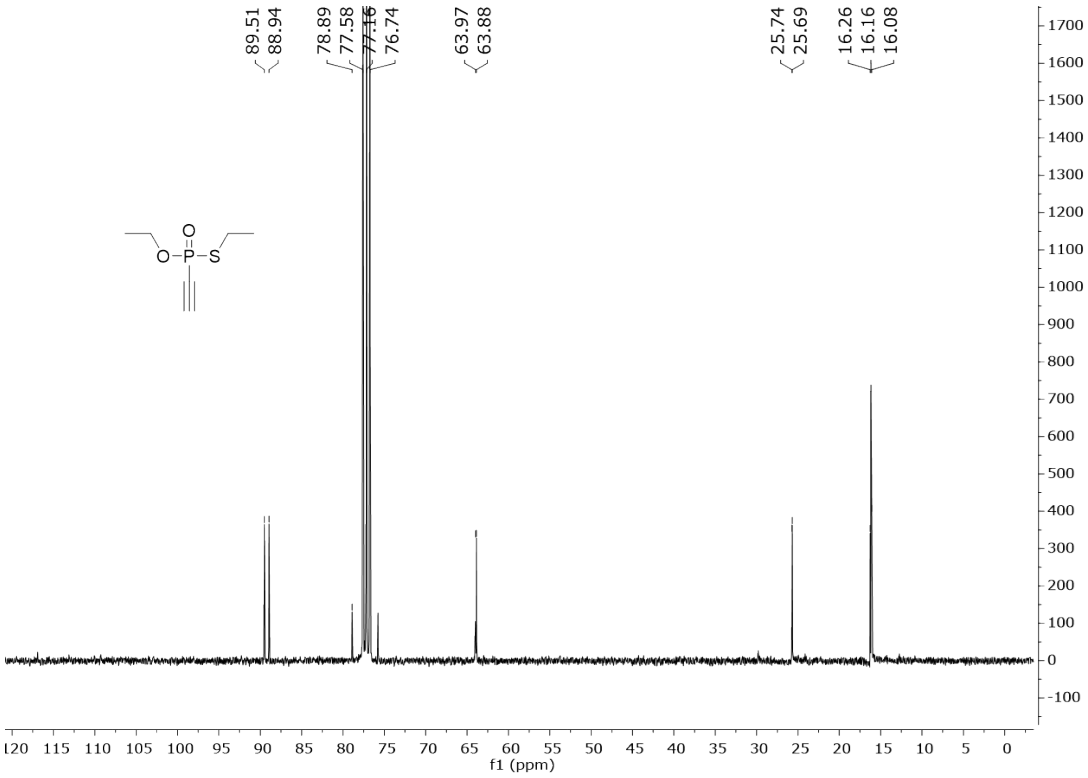

^{31}P-NMR spectrum of compound **13** in $CDCl_3$ (122 MHz):

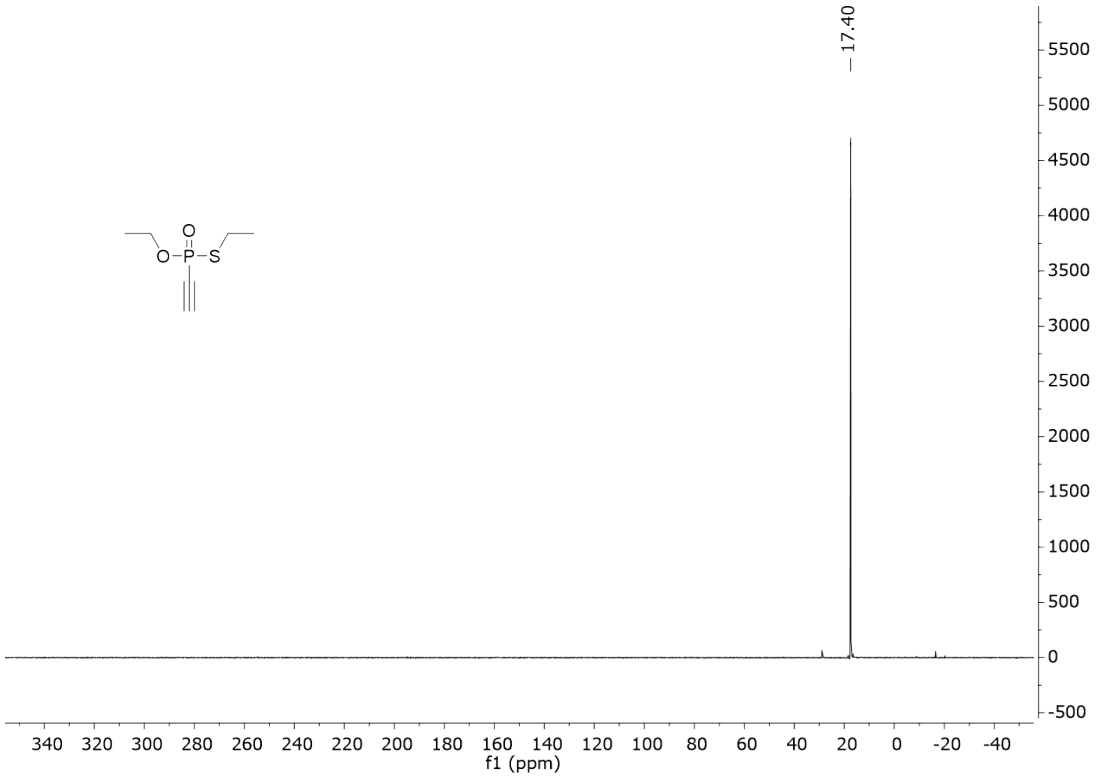

^{1}H-NMR spectrum of compound **18** (*Z*-isomer) in D_2O (600 MHz):

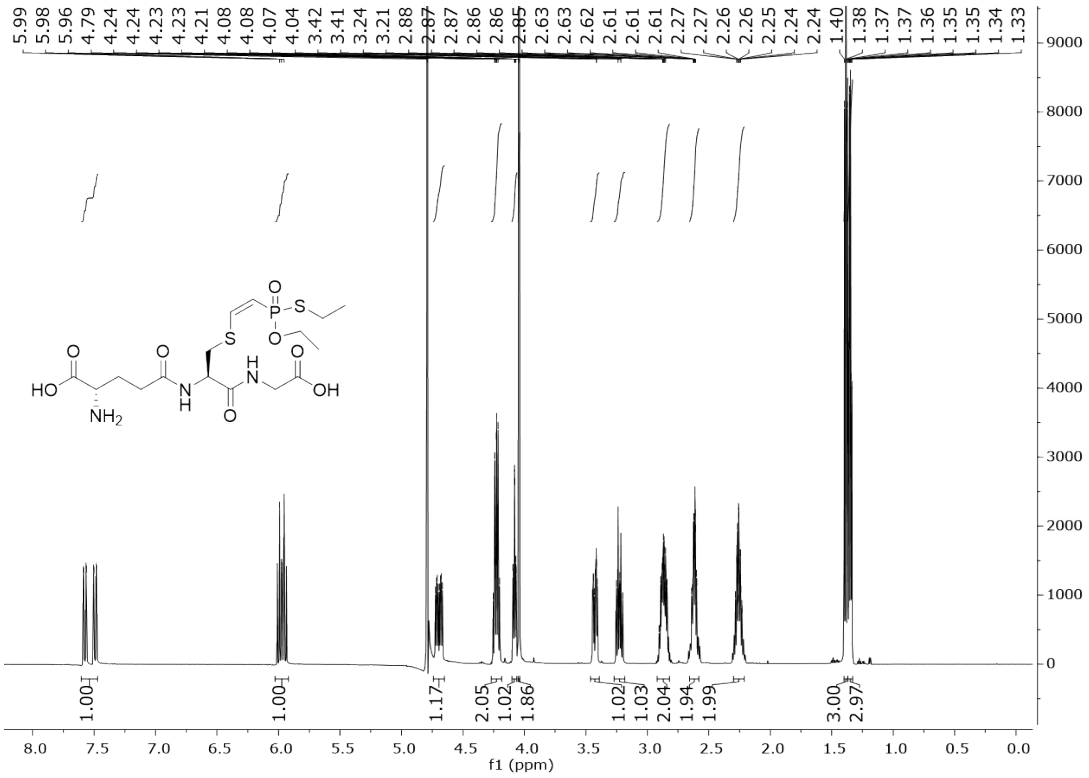

^{13}C-NMR spectrum of compound **18** (*Z*-isomer) in D_2O (151 MHz):

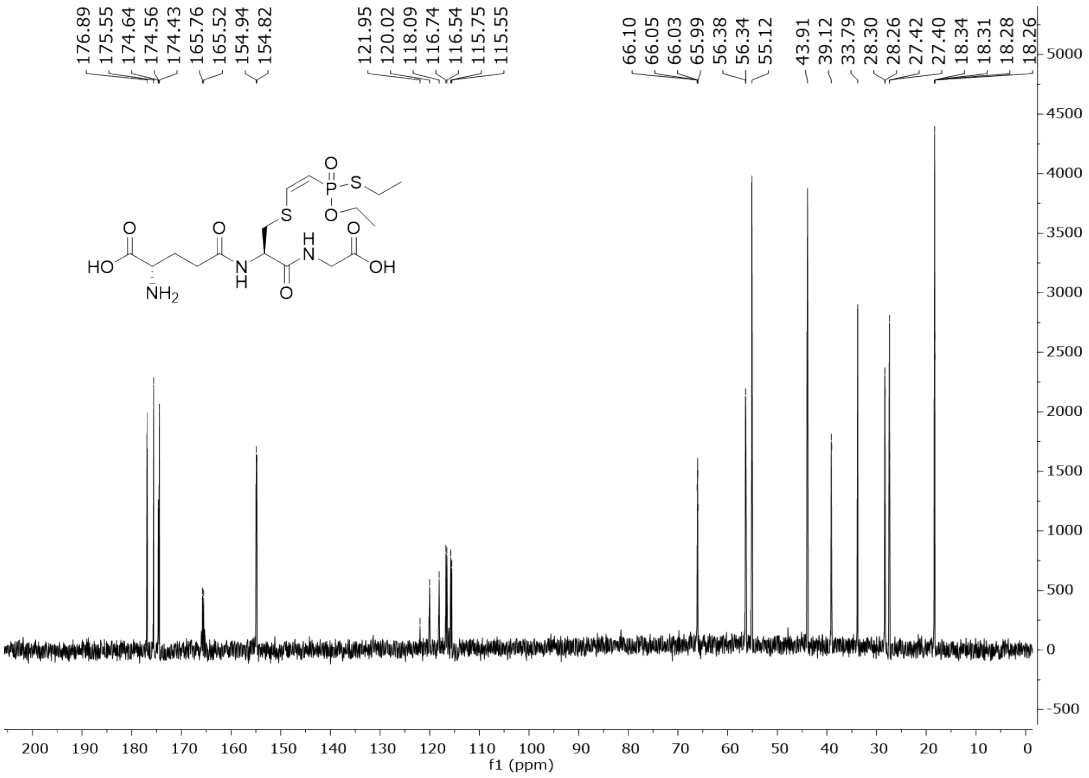

^{31}P-NMR spectrum of compound **18** (*Z*-isomer) in D_2O (243 MHz):

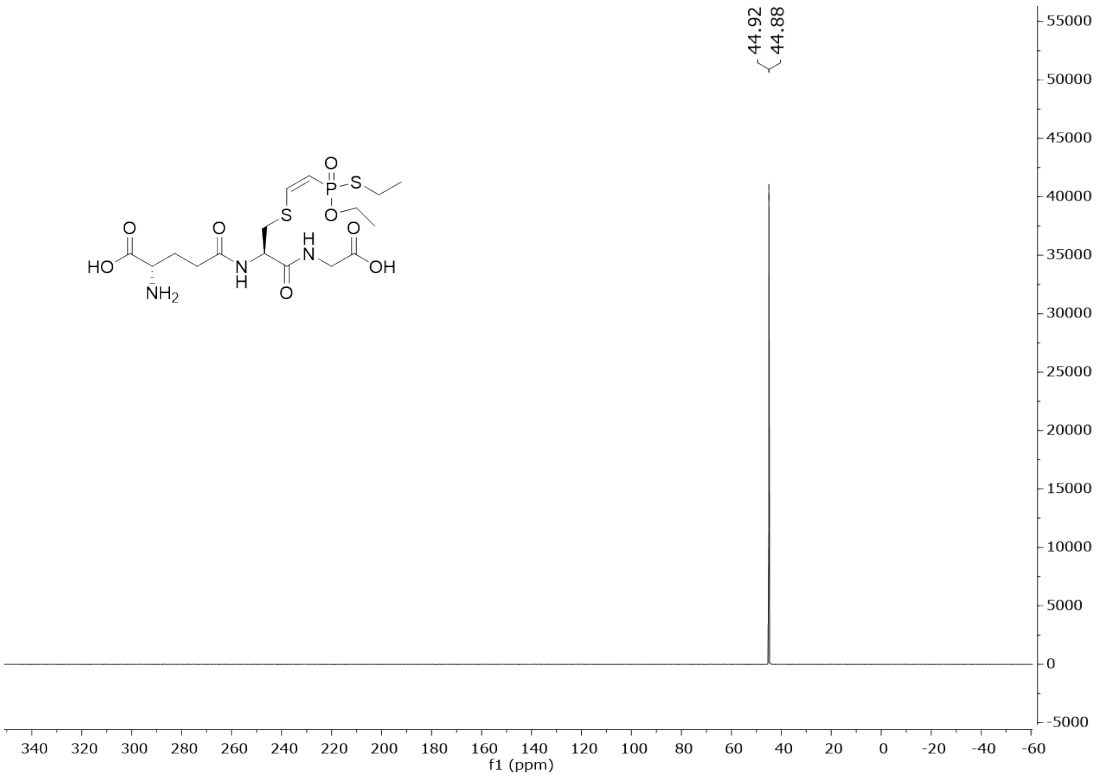

^{1}H-NMR spectrum of compound **18** (*E*-isomer) in D_2O (600 MHz):

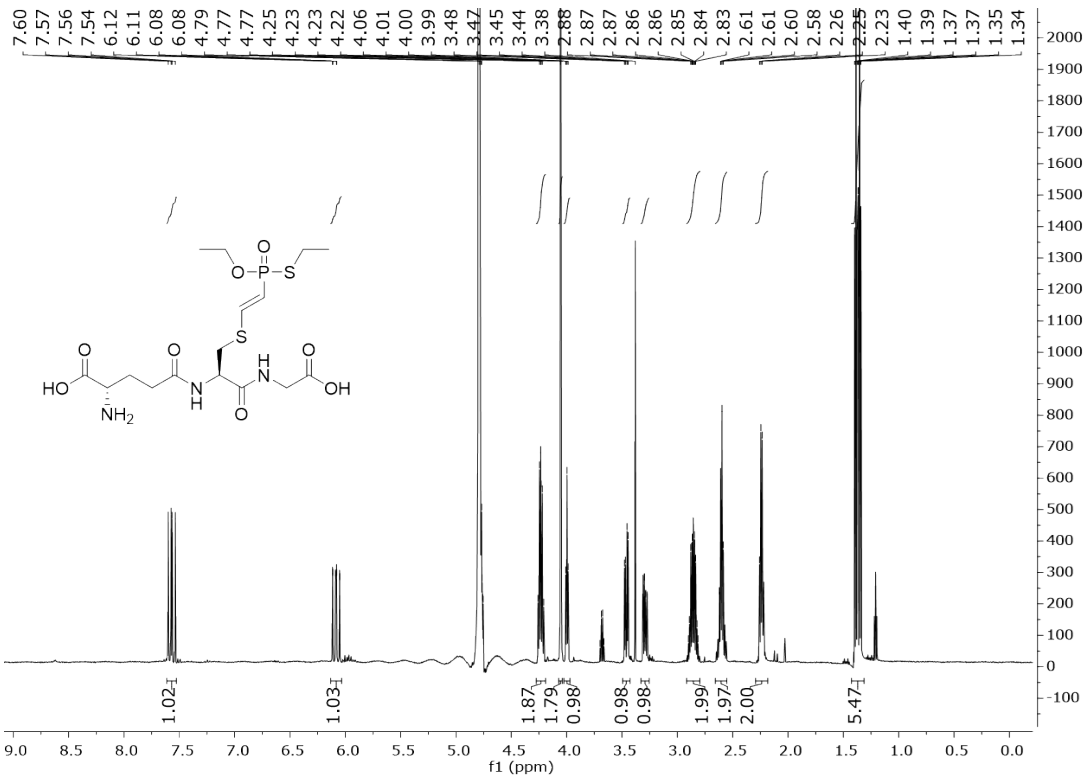

^{13}C-NMR spectrum of compound **18** (*E*-isomer) in D_2O (151 MHz):

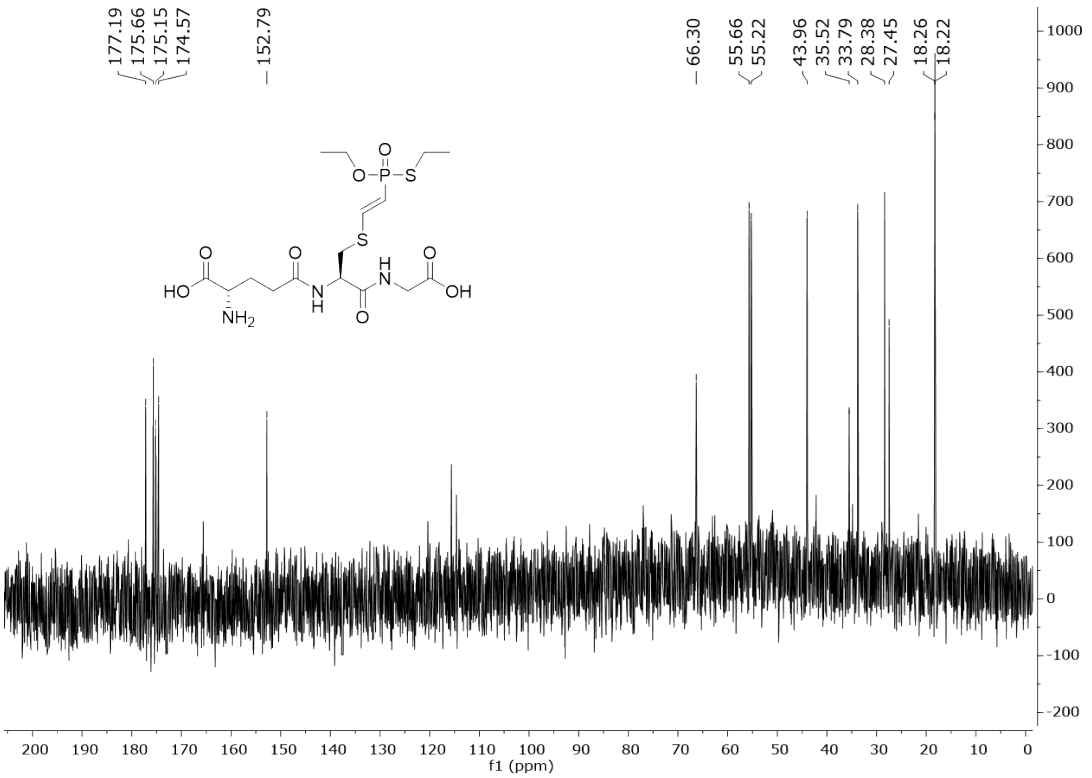

^{31}P-NMR spectrum of compound **18** (*E*-isomer) in D_2O (243 MHz):